CZECH TECHNICAL UNIVERSITY
Faculty of Civil Engineering
Department of Steel and Timber Structures

UNIVERSITY OF AVEIRO
Department of Civil Engineering

Stainless steel structures deformation

Master's Thesis

Bc. Ondřej Mohr

Supervisors:

prof. Dr. Nuno Lopes

prof. Ing. Michal Jandera, Ph.D.

Aveiro, January 2023

ČESKÉ VYSOKÉ UČENÍ TECHNICKÉ V PRAZE
Fakulta stavební
Thákurova 7, 166 29 Praha 6

ZADÁNÍ DIPLOMOVÉ PRÁCE

I. OSOBNÍ A STUDIJNÍ ÚDAJE

Příjmení: Mohr Jméno: Ondřej Osobní číslo: 477496

Zadávající katedra: Katedra ocelových a dřevěných konstrukcí

Studijní program: Stavební inženýrství

Studijní obor/specializace: Konstrukce pozemních staveb

II. ÚDAJE K DIPLOMOVÉ PRÁCI

Název diplomové práce: Průhyb konstrukcí z korozivzdorných ocelí

Název diplomové práce anglicky: Stainless steel structures deformation

Pokyny pro vypracování:
The thesis will be focused on a numerical study of deflection of stainless-steel structures, such as beams, portal frames and trusses. The numerical models used in the study will be validated on experimental results from literature. Design procedures in European standards and literature (i.e. Real and Mirambell) will be compared and if possible, more accurate procedures will be proposed.

The thesis will be written in English.

Seznam doporučené literatury:
EN 1993-1-4
E Mirambell, E Real, On the calculation of deflections in structural stainless steel beams: an experimental and numerical investigation, Journal of Constructional Steel Research, Vol 54, 2000, p 109-133.
SCI, Design manual for structural stainless steel, Ascot, Berkshire, UK : Steel Construction Institute, 2017.

Jméno vedoucího diplomové práce: Michal Jandera

Datum zadání diplomové práce: 22.8.2022 Termín odevzdání DP v IS KOS: 9.1.2023
Údaj uveďte v souladu s datem v časovém plánu příslušného ak. roku

Podpis vedoucího práce Podpis vedoucího katedry

III. PŘEVZETÍ ZADÁNÍ

Beru na vědomí, že jsem povinen vypracovat diplomovou práci samostatně, bez cizí pomoci, s výjimkou poskytnutých konzultací. Seznam použité literatury, jiných pramenů a jmen konzultantů je nutné uvést v diplomové práci a při citování postupovat v souladu s metodickou příručkou ČVUT „Jak psát vysokoškolské závěrečné práce“ a metodickým pokynem ČVUT „O dodržování etických principů při přípravě vysokoškolských závěrečných prací“.

Datum převzetí zadání Podpis studenta(ky)

ČESKÉ VYSOKÉ UČENÍ TECHNICKÉ V PRAZE
Fakulta stavební
Thákurova 7, 166 29 Praha 6

SPECIFIKACE ZADÁNÍ

Jméno diplomanta: Ondřej Mohr

Název diplomové práce: Průhyb konstrukcí z korozivzdorných ocelí

Základní část: Ocelové konstrukce podíl: 100 %

Formulace úkolů: viz zadání

Podpis vedoucího DP: .... Datum: ....

Případné další části diplomové práce (části a jejich podíl určí vedoucí DP):

2. Část: podíl: %

Konzultant (jméno, katedra):

Formulace úkolů:

Podpis konzultanta: .... Datum: ....

3. Část: podíl: %

Konzultant (jméno, katedra):

Formulace úkolů:

Podpis konzultanta: .... Datum: ....

4. Část: podíl: %

Konzultant (jméno, katedra):

Formulace úkolů:

Podpis konzultanta: .... Datum: ....

Declaration

I hereby declare that I have written this master's thesis independently and quoted all the sources of information used in accordance with methodological instructions on ethical principles for writing an academic thesis. Moreover, I state that this thesis has neither been submitted nor accepted for any other degree.

In Aveiro, January 2023

....

Bc. Ondřej Mohr

Acknowledgements

I would like to thank my supervisors, prof. Dr. Nuno Lopes and prof. Ing. Michal Jandera, Ph.D. for their professional guidance in developing this thesis.

Abstrakt

Tato diplomová práce je zameřena na studii deformací konstrukcí z korozivzdorné oceli. Byly vytvořeny numerické modely prostých nosníků v MKP softwaru Abaqus, které byly validovány na výsledcích experimentů z literatury. Byla ověřena stávající metoda návrhu konstrukcí podle Eurokódu a také přesnější metody pro výpočet průhybů prostých nosníků (metoda navržená prof. E. Realovou a prof. E. Mirambellem, metoda uvedená v čínské normě). Deformace vypočtené těmito metodami byly porovnány s těmi, jež byly získány z numerických modelů. Následně byla navržena nová přibližná metoda stanovení průhybů, jejíž použití bylo rozšířeno i na výpočet deformací portálových rámů. Dále byl stanoven postup pro výpočet průhybů konstrukcí s osově namáhanými prvky (ztužené portálové rámy, příhradové vazníky).

Klíčová slova

nerezová ocel, deformace, průhyb, nosník, příhradový vazník, rám, rám se ztužidlem, numerické modelování, nelineární pracovní diagram, mezní stav použitelnosti

Abstract

This master's thesis is focused on the study of deformations of stainless steel structures. Numerical models of simply supported beams were created in FEM code Abaqus and validated on the results of experiments from the literature. The current design method provided in the Eurocode was verified, as well as more accurate methods for calculating deflections of simply supported beams (method proposed by prof. E. Real and prof. E. Mirambell, method provided in Chinese code). The deflections calculated with these methods were compared to those obtained from numerical models. Furthermore, a new approximate method for estimating deflections was proposed and its usage was extended to the calculation of deflections of portal frames. Moreover, a procedure for the calculation of deflections of truss structures (braced portal frames, truss beams) was proposed.

Keywords

stainless steel, deformation, deflection, beam, truss, portal frame, braced portal frame, numerical modeling, non-linear stress-strain diagram, serviceability limit state

Contents

1 Introduction

Stainless steel is an iron alloy with increased resistance against chemical and electrochemical corrosion. This resistance is caused by high chromium content, which creates a protective layer, causing the typical metallic-looking surface. This layer is also able to self-repair when damaged. Stainless steel can be divided into three basic families: austenitic steel, ferritic steel, and duplex steel.

The usage of stainless steel in construction has increased in the past years due to its corrosion resistance and low requirements for maintenance. However, this material is very expensive compared to carbon steel, and therefore its usage in construction is limited.

2 Current state of design procedures

The design of stainless steel structures has the same principle as for carbon steel, however, the rules are different for cases, where the stress-strain diagram must be taken into account, such as stability or calculation of deflections.

The stress-strain relationship for carbon steel is considered to be linear up to the yield stress. This relationship is given by Hooke's law (1).

$$\varepsilon = \frac{\sigma}{E} \tag{1}$$

where ε is the strain, σ is the stress, and E is Young's modulus of elasticity.

Unlike carbon steel, the stress-strain curve for stainless steel is always non-linear and doesn't show a clearly defined yield strength point. Therefore, the yield strength is generally considered as 0.2 % proof stress. Figure 1 shows typical stress-strain curves for the austenitic, ferritic, and duplex steel.

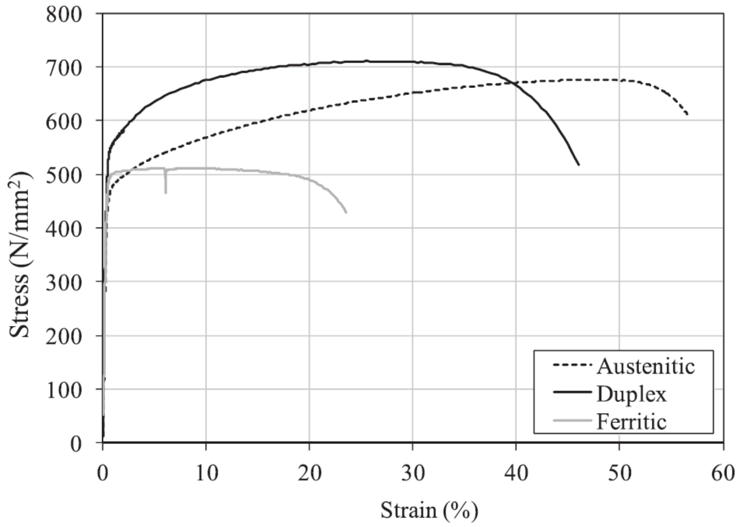

Figure 1: Typical stress-strain curves for austenitic, ferritic and duplex steel [3]

2.1 Description of stress-strain curves

Ramberg-Osgood model, which has been originally proposed for aluminum alloys was later extended for stainless steel. The two-stage model, given by (2) and (3), is able to accurately describe the stress-strain relationship for stress levels both below and above the yield strength.
for $\sigma \leq f_y$:

$$\varepsilon = \frac{\sigma}{E_0} + 0.002 \left(\frac{\sigma}{f_y}\right)^n \tag{2}$$

for $\sigma > f_y$:

$$\varepsilon = \frac{\sigma - f_y}{E_{0.2}} + \left(\epsilon_u - \epsilon_{t,0.2} - \frac{f_u - f_y}{E_{0.2}}\right) \left(\frac{\sigma - f_y}{f_u - f_y}\right)^m \tag{3}$$

where E_0 is the initial Young's modulus, f_y is the yield stress corresponding to 0.2% of plastic strain, f_u is the ultimate tensile stress, E_0 is the tangent modulus at the 0.2% proof stress, ε_u is the strain at the ultimate tensile stress and n and m are model parameters.

2.2 Design procedures according to EN 1993-1-4

According to Eurocode 3, Part 1-4 [4], deflections of stainless steel members are supposed to be determined by using the secant modulus of elasticity E_{secant}. Using the Ramberg-Osgood equation, E_{secant} can be calculated with:

$$E_{secant} = \frac{E_0}{1 + 0.002\,\frac{E_0}{\sigma_{ser}}\left(\frac{\sigma_{ser}}{f_y}\right)^n} \tag{4}$$

where σ_{ser} is the design value of stress in the serviceability limit state.

The value of the secant modulus is variable along the member and also over the height of the cross-section. Due to the lack of accurate design procedure, Eurocode 3, Part 1-4 offers a simplified method, where the minimum value of secant modulus, corresponding to the maximum value of stress in the member, is used.

For the determination of deflections of simply supported beams subjected to basic load cases, Eurocode refers to the *Design manual for stainless steel* [8], which contains a method proposed by Real and Mirambell [7]. This method is described in more detail in 2.3.

2.3 Design method proposed by Real and Mirambell

Since the method for calculation of deflections described in Eurocode considers a unique value of Young's modulus, the deflections are overestimated. The magnitude of over-estimation rises with higher levels of stress and also depends on moment distribution along the member.

The method proposed by E. Real and E. Mirambell [7] takes into account the variation of Young's modulus both along the member length and over the height of the cross-section and therefore offers a more accurate estimation of deflections of simply supported beams.

This method uses a moment-curvature relationship and estimates the deflections by direct integration. This relationship is calculated as an elastic curvature with the addition of a plastic component:

$$\chi = \frac{M}{EI} + \chi_p \left(\frac{M}{M_{0.2}}\right)^{n-1} \tag{5}$$

where χ is the curvature, M is the applied bending moment, I is the second moment of area, $M_{0.2}$ is the applied bending moment when the stress in the extreme fibers reaches the yield stress and χ_p is the plastic curvature for $M_{0.2}$ determined by:

$$\chi_p = \frac{2}{h}\left(\frac{f_y}{E} + 0.002\right) - \frac{M_{0.2}}{EI} \tag{6}$$

where h is the height of the cross-section.

The maximum bending moment $M_{0.2}$ can be either calculated as an elastic moment of resistance or more accurately, using (7) and (8). These equations consider the non-linear distribution of stress over the height of the cross-section and the obtained moments of resistance are approximately 10-20 % higher.

For SHS and RHS cross-sections:

$$M_{0.2} = f_y t(b-2t)(h-t) + h^3\chi_{0.2}2t\left[\frac{E}{12} - \frac{0.002E\chi_{0.2}h}{32\left(\frac{f_y}{E}+0.002\right)^2}\right] \tag{7}$$

For I cross-sections:

$$M_{0.2} = f_y t(b-t_w)(h-t_f) + h^3\chi_{0.2}t_w\left[\frac{E}{12} - \frac{0.002E\chi_{0.2}h}{32\left(\frac{f_y}{E}+0.002\right)^2}\right] \tag{8}$$

where b is the width of the cross-section, t is the thickness of the plate, t_w is the thickness of the wall, t_f is the thickness of the flange and $\chi_{0.2}$ is the maximum curvature, calculated with:

$$\chi_{0.2} = \frac{2}{h}\left(\frac{f_y}{E} + 0.002\right) \tag{9}$$

For simply supported beams with symmetrical bending moment law, the deflections can be estimated with direct integration:

$$d = \int_0^{L/2}\chi(x)xdx = \int_0^{L/2}\frac{M(x)x}{EI}dx + \int_0^{L/2}\chi_p\left(\frac{M(x)}{M_{0.2}}\right)^{n-1}xdx \tag{10}$$

where x is the longitudinal coordinate of the beam.

For basic load cases (concentrated load at mid-span, uniform bending moment, uniformly distributed load) the elastic deflections (I_1) and plastic deflections (I_2)

are estimated in Tab. 1.

Table 1: Estimation of deflections of simply supported beams subjected to basic load cases provided in [8]

Load case	I_1	I_2
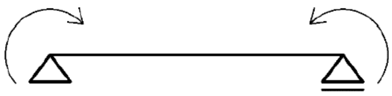	$\frac{ML^2}{8EI}$	$\chi_p \left(\frac{M}{M_{0.2}}\right)^{n-1} \left(\frac{L^2}{8}\right)$
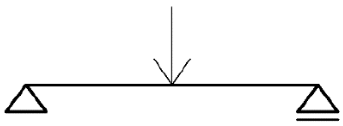	$\frac{PL^3}{48EI}$	$\chi_p \left(\frac{F}{2M_{0.2}}\right)^{n-1} \left(\frac{(L/2)^{n+1}}{n+1}\right)$
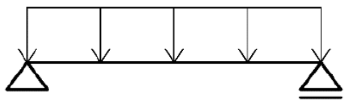	$\frac{5fL^4}{384EI}$	$\chi_p \left(\frac{f}{2M_{0.2}}\right)^{n-1} L^{2n} 0.1 e^{-1.45(n-1)}$

2.4 Method provided in the Chinese code

The method provided in the Chinese code CECS 410 [1] is similar to the one proposed by Real and Mirambell, as it also uses a direct integration of the moment-curvature relationship. The curvature is calculated by (11) and formulas for determining deflections of beams subjected to the three previously mentioned load cases are shown in Tab. 2.

$$\chi = \frac{M}{EI} + \frac{0.004}{h} \left(\frac{M}{M_{0.2}}\right)^n \tag{11}$$

Calculation of the moment of resistance $M_{0.2}$ is done with method proposed in [5], which uses coefficient β_{pro}, which is a ratio between $M_{0.2}$ for rectangular cross-section and the elastic moment of resistance. This coefficient can be calculated by (12).

$$\beta_{pro} = 1.56 - 4.5\sqrt{\frac{f_y}{E_0}} - \frac{0.6}{n} \tag{12}$$

Furthermore, the moment of resistance for I cross-sections is calculated by (13). The Chinese code lacks a procedure for RHS cross-sections.

$$M_{0.2,pro} = f_y t_f (b - t_w)(h - t_f) + \beta_{pro} f_y t_w \frac{h^2}{6} \tag{13}$$

Table 2: Estimation of deflections of simply supported beams subjected to basic load cases provided in the Chinese code [1]

Load case	Deflection
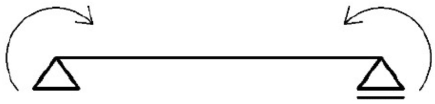	$\frac{ML^2}{8EI} + \frac{0.004}{h}\left(\frac{M}{M_{0.2}}\right)^n \frac{L^2}{8}$
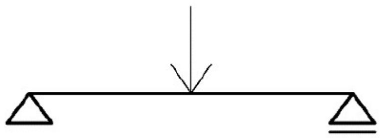	$\frac{FL^3}{48EI} + \frac{0.004}{h}\left(\frac{FL}{4M_{0.2}}\right)^n \frac{L^2}{4(n+2)}$
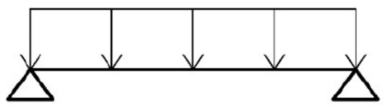	$\frac{fL^4}{384EI} + \frac{0.004}{h}\left(\frac{fL^2}{2M_{0.2}}\right)^n \frac{L^2}{10} e^{-1.45n}$

3 Numerical model

3.1 Analysis and element type

The finite-element code Abaqus 2020 was used to create numerical models of analyzed structures.

The element type used is B31 (linear beam element in three-dimensional space). According to [2], in order to receive acceptable results from the beam theory, the cross-section dimensions should be less than 1/10 of the axial dimension of the model. The beam section types used were I sections for creating I and H cross-sections and BOX sections for creating hollow (RHS, SHS) cross-sections. The through-thickness integration was accomplished with Simpson's rule of order five. The layout of integration points is shown in Fig. 2.

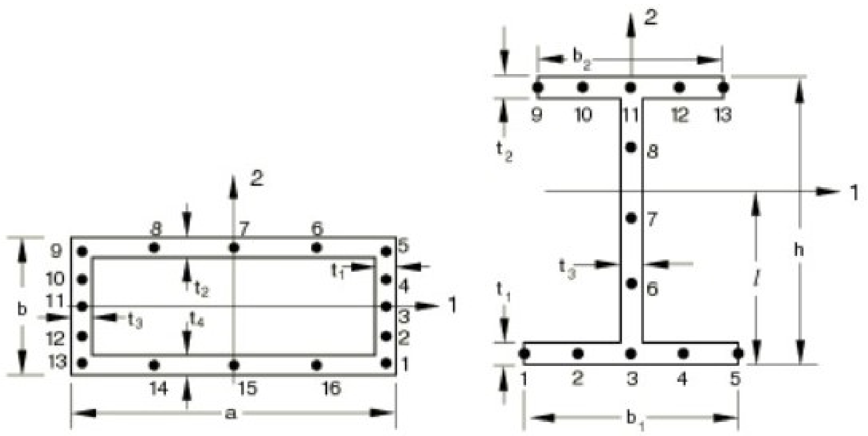

Figure 2: Integration points display of I and BOX sections [2]

The analysis involves a static problem with a non-linear material and the Newton–Raphson method is used. The mesh density used was 1000 elements per one simply supported beam and 100 elements per member in more complicated structures (frames, trusses). A lower density would be sufficient for reliable results, however, since the deflections are retrieved in the nodes only, a higher density is required, otherwise, the point of the maximum deflection might be missed.

Linear analysis of simply supported beams was done in MS Excel. Linear analysis of other structures was done in Dlubal RFEM5 software. The mesh density was set to a minimum of 10 elements per member. The analysis was done using the Newton-Raphson method.

It is important to mention, that the potential effect of local buckling of Class 4 sections is not taken into account when using beam elements.

3.2 Material

The stress-strain relationship of the material has been modeled as a multi-linear curve, whose points were obtained from (2). Since all models were loaded until yield strength, it was not necessary to use the second stage of the compound Ramberg-Osgood diagram (3). The material is considered to behave elastically up to a stress value of 50 MPa. The elastic behavior is represented by the value of Young's modulus equal to 200 GPa and Poison's ratio equal to 0.3. Values of n and f_y for each type of steel used in this study are shown in Tab. 3.

Table 3: Material properties - taken from [4]

Steel	Grade	n	f_y (MPa)
Austenitic	1.4301	7	230
Ferritic	1.4003	14	280
Duplex	1.4462	8	480

3.3 Validation of numerical model

The numerical model has been validated on the results from tests performed in Barcelona [6], during which three simply supported beams of different types of cross-sections (square hollow section 80×80×3, rectangular hollow section 80×120×4, H-section 100×100×8) were subjected to a concentrated load at mid-span. Furthermore, the deflections of tested beams were calculated using the Eurocode procedure for comparison.

Mechanical properties, which have been found from tests on specimens derived from the profiles, are shown in Tab. 4. In order to validate the numerical model, these properties were then input into the Abaqus code.

Table 4: Mechanical properties of tested specimens

Profile tested	f_y (MPa)	E_0 (GPa)	n	σ_{max} (MPa)
SHS 80×80	422	165.57	4.80	944
RHS 80×120	442	161.16	6.16	925
H 100×100	414	160.11	6.37	834

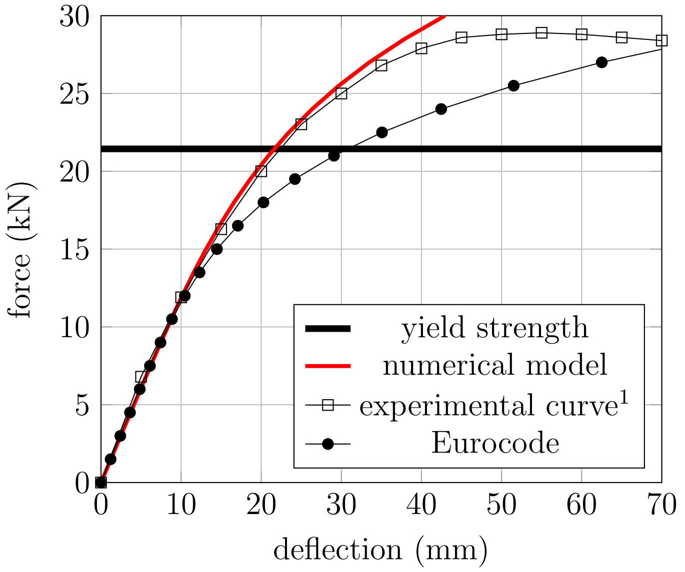

Figure 3: Load-deflection curve for SHS 80×80×3 simply supported beam with a span length of 1800 mm

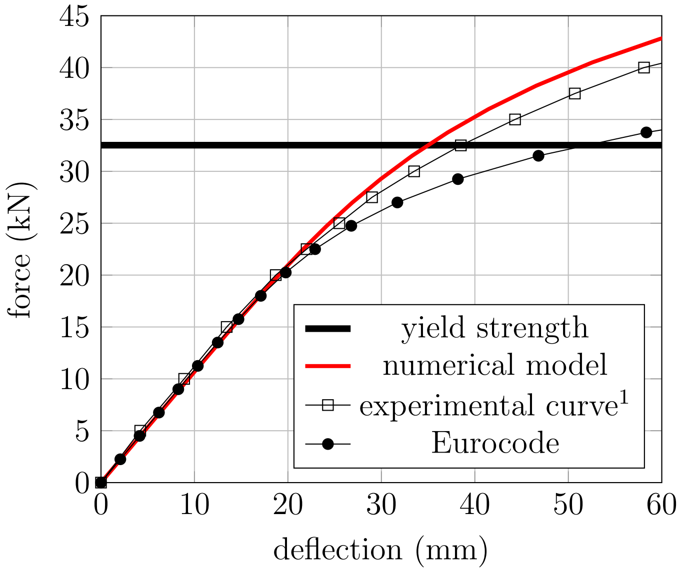

Figure 4: Load-deflection curves for RHS 80×120×4 simply supported beam with a span length of 2800 mm

[1]Points on the curves were extracted from the image in [6].

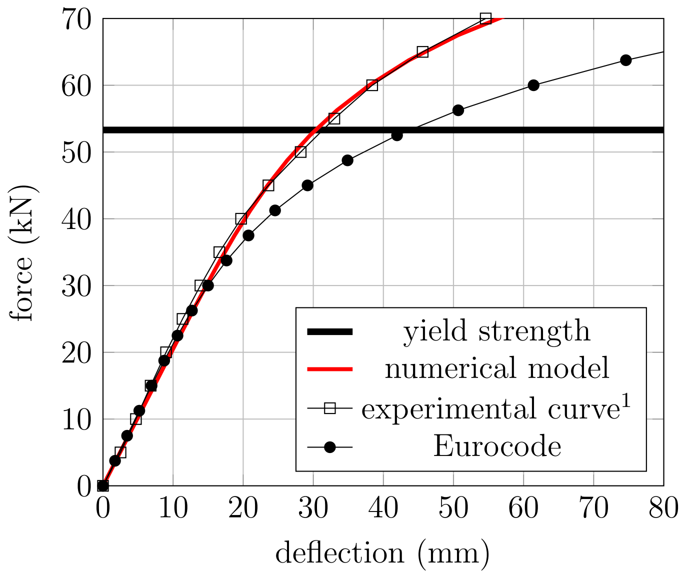

Figure 5: Load-deflection curves for H 100×100×8 simply supported beam with a span length of 2400 mm

Figs. 3 to 5 show a comparison of deflections calculated with the numerical model with those from literature [6]. The results are very similar, however, deflections are slightly underestimated in the cases of SHS and RHS beams. This might be caused by the fact, that these cross-sections are classified as Class 4, which might lead to a local buckling effect. Local buckling, as mentioned above, is not taken into account, when using the beam finite elements.

It can be observed, that deflections calculated by Eurocode are overestimated for higher levels of stress. The accuracy of this method is further examined in 4.1.

Since the numerical model describes the material behavior very accurately and the results are in a very good match with those measured during experiments, the model is considered validated and deflections obtained from it are considered as actual deflections in further research.

4 The author's research preceding the master's thesis

This thesis was preceded by the author's research within the P04C subject focused on the study of deflections of stainless steel structures, such as simply supported beams and braced portal frames. In the case of simply supported beams, results obtained from previously presented methods were compared to those obtained from numerical models and also to experimental results from literature [6].

4.1 Deflections of simply supported beams

Deflections of simply supported beams of various cross-sections were estimated by a method provided in the Eurocode (using E_{secant}), a method proposed by Real and Mirambell ("**R&M**" using an elastic moment of resistance and "**R&M-modified**" using a moment of resistance calculated by (7) and (8)) and a method provided in the Chinese code (**CECS 410**) and the results were compared to those obtained from the numerical model. Beams were subjected to three basic load cases (uniformly distributed bending moment, concentrated load at mid-span, uniformly distributed load). Considering the amount of data, results for representative profiles (I 200×100, RHS 120×80) are shown only. The properties of studied beams are described in Tab. 5.

Figs. 6 and 7 confirm the previous statement, that the deflections calculated according to the Eurocode are overestimated for higher levels of stress. The method proposed by Real and Mirambell using an elastic moment of resistance (**R&M**) shows more accurate results for load cases of a concentrated load at mid-span and uniformly distributed load. However, in the case of uniform bending moment, deflections are similar to those calculated by the method provided in the Eurocode. The same method with a modified moment of resistance (**R&M-modified**) and the method provided in CECS 410 give the most accurate results, nevertheless, they are slightly underestimated. Furthermore can be stated, that for levels of stress, that do not reach over 50 % of the yield strength, behavior is linear, therefore deflections can be calculated using the initial Young's modulus E_0.

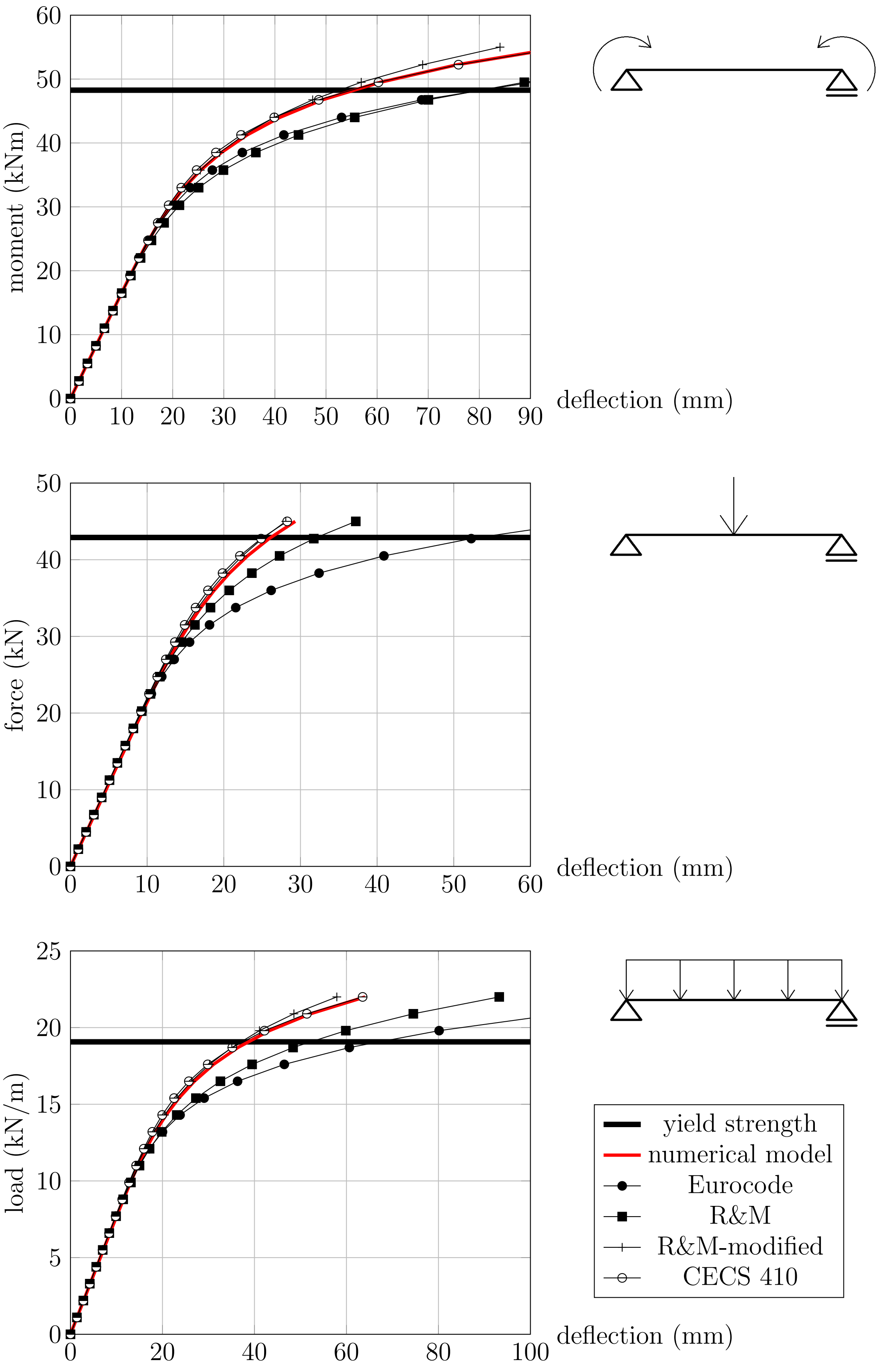

Figure 6: Load-deflection curves for I 200×100 cross-section

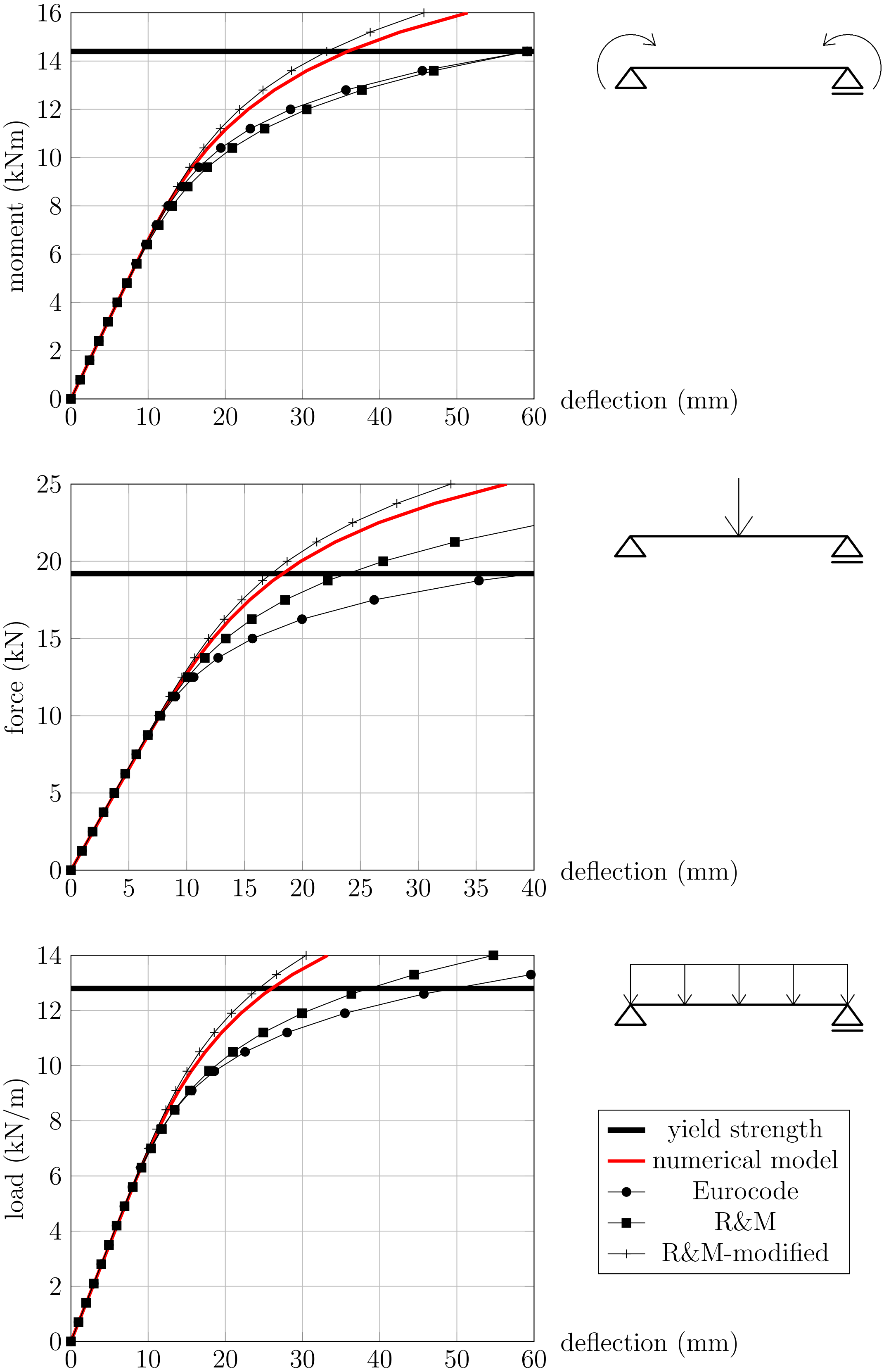

Figure 7: Load-deflection curves for RHS 120×80 cross-section

Table 5: Properties of studied beams

Profile	Total depth (mm)	Flange width (mm)	Flange thickness (mm)	Web thickness (mm)	Span length (mm)	Material
I	200	100	10	6	4500	1.4301
RHS	120	80	5	5	3000	1.4301

4.2 Braced portal frames

Several portal frames with bracings subjected to two equal horizontal forces were analyzed in the Abaqus code. Obtained horizontal deflections (**Abaqus deflections** - calculated by materially nonlinear analysis) of the tops of the columns were compared to those calculated by linear analysis, using Dlubal RFEM5 software. Three different deflections were obtained from this software (**linear deflection** - using the initial Young's modulus E_0, **Eurocode deflection** - using the same secant modulus for the entire structure, calculated by (4), σ_{ser} is the maximum magnitude of stress on the structure, **Modified deflection** - using different secant moduli for the frame and for the bracings separately, calculated by (4), σ_{ser} is the maximum magnitude of stress on each part of the structure (frame, bracings).

Models of three portal frames were created. In the first model, the cross-sections were set so that the stress reached the yield strength at both the frame and the bracings, in the second model, the yield strength is reached at the frame only and in the third model, the yield strength is reached at the bracings only. The loading scheme is shown in Fig. 8. and cross-sections are described in Tab. 6. The stress distribution is shown in Fig. 9. The material used for all frames is 1.4301.

Table 6: Cross-sections of analyzed frames

Frame	Columns[2]	Girder[2]	Bracings[3]
Fr. 1	I 100/50/8.4/3	I 100/50/5.5/3	CHS 100/6.5
Fr. 2	I 100/50/9/5	I 100/50/3.1/3	CHS 150/8
Fr. 3	I 100/50/8/3	I 100/50/8/3	CHS 70/4

[2]Explanation of I cross-section dimensions: I $h/b/t_f/t_w$
[3]Explanation of CHS cross-section dimensions: CHS d/t

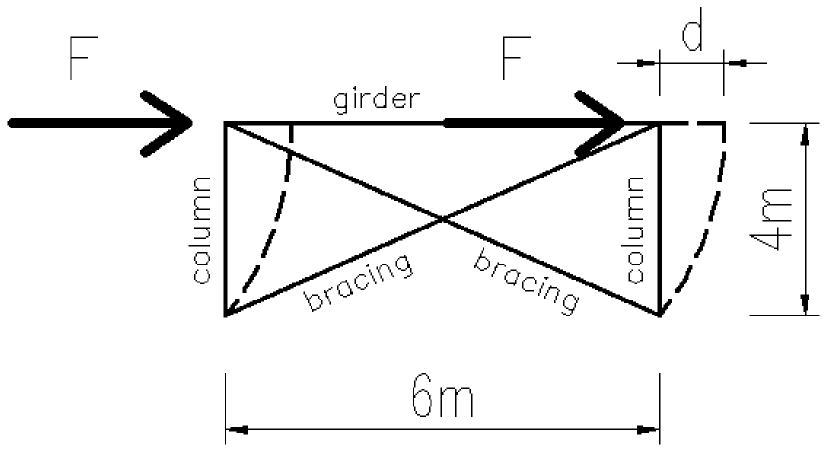

Figure 8: Load scheme of analyzed portal frames

The results are shown in Tab. 7 for load steps corresponding to 60 %, 80 % and 100 % of the magnitude of loading forces, where 100 % of the force magnitude leads to maximum stress on the structure equal to the yield strength.

Table 7: Results - horizontal deflections of braced portal frames

Frame	Load step	Force [kN]	Elastic defl. [mm]	Abaqus defl. [mm]	Eurocode defl. [mm]	Modified defl. [mm]
Fr. 1	60 %	220	7.81	8.44	8.47	8.47
	80 %	293	10.40	15.09	15.30	15.30
	100 %	366	12.98	35.00	35.59	35.59
Fr. 2	60 %	272	5.83	6.01	6.34	5.99
	80 %	362	7.75	9.13	11.53	9.16
	100 %	453	9.60	16.12	26.58	16.06
Fr. 3	60 %	95	6.77	7.32	7.32	7.26
	80 %	127	9.06	12.81	13.19	12.69
	100 %	159	11.30	28.71	31.06	28.69

σ [MPa]:

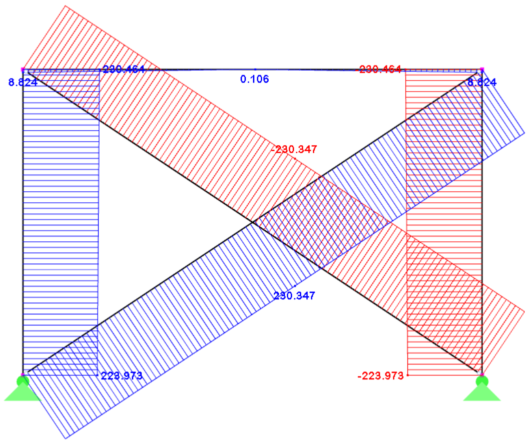

(a) Frame Fr. 1

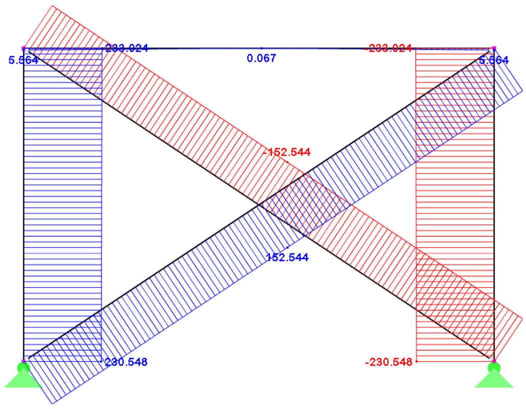

(b) Frame Fr. 2

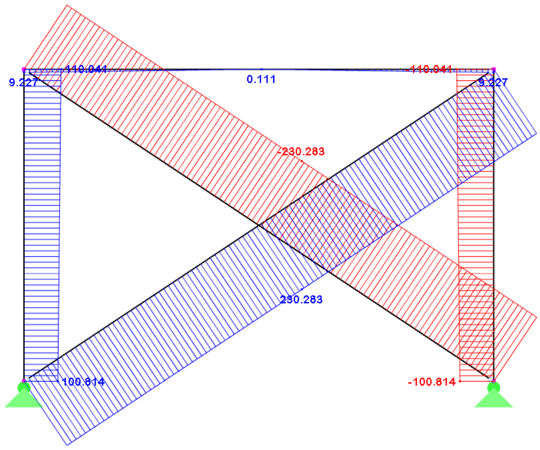

(c) Frame Fr. 3

Figure 9: Stress distribution fof analyzed frames subjected to 100 % of loading forces

In conclusion can be stated, that similarly to simply supported beams, the effect of non-linearity must be taken into account for braced portal frames, in which the maximum stress reaches more than approximately 50 % of the yield strength. When following the Eurocode design procedure, where the secant modulus is calculated based on the maximum magnitude of stress and applied for the entire structure, the results are satisfying, however, they may be over-estimated for cases with less stressed bracings. The modified deflections show the closest match with the numerical model.

5 New method

As can be observed in 4.1, the most accurate deflections of simply supported beams are calculated by the method provided in CECS 410 and by the method proposed by Real and Mirambell using the modified moment of resistance. However, since the calculation procedure is lengthy and the methods can only be used for a few basic cases, a new method is proposed below.

The newly proposed method simplifies the variation of Young's modulus over the height of the cross-section by splitting the cross-section into flanges and web(s) and determining the secant modulus separately for each part. Since the moment of inertia of the flanges is usually very different from the one of the web(s), it is a good approximation to reduce the contribution of each part to the overall bending stiffness of the cross-section by using two different secant moduli of elasticity.

In the first step, numerical models consisting of flanges/webs only were created and loaded by uniform bending moments. Then, obtained deflections were compared to those calculated using the secant modulus of elasticity, which was calculated by (4). When considering the value of σ_{ser} as the maximum stress, the deflections are overestimated, since this procedure is very similar to the one stated in the Eurocode. Therefore, the value of the stress used for E_{ser} calculation is not considered at the extreme fibers, but at a particular point in the cross-section, closer to the neutral axis.

5.1 Flanges

After comparing results obtained from several numerical models, the value of $\sigma_{ser,fl}$ for calculating the secant modulus for flanges has been determined as the value of stress at 1/3 of the thickness of the flange, as shown in Fig. 10. This value can be calculated by (14). The stress distribution is considered to be linear. Considering this value of stress, the deflections are very accurate and never underestimated for commonly used cross-sections.

$$\sigma_{ser,fl} = \sigma_{max} \cdot \frac{h - \frac{2}{3} \cdot t_f}{h} \tag{14}$$

where $\sigma_{ser,fl}$ is the value of stress used for calculation of $E_{secant,fl}$ by (4) and σ_{max} is the value of stress at the extreme fibers.

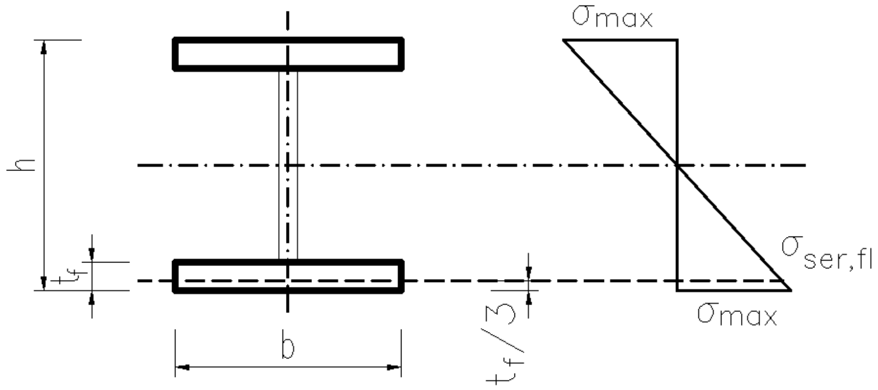

Figure 10: Stress distribution considered for calculation of the secant modulus of flanges

Figs. 11 and 12 show deflections estimated elastically using $E_{secant,fl}$, compared to those obtained from a numerical model. Results for other analyzed cross-sections can be found in the Annex (Figs. 33 and 34).

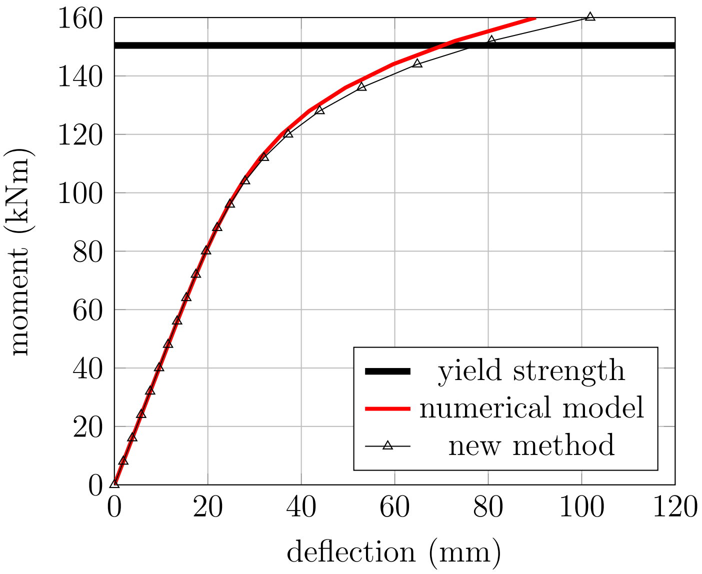

Figure 11: Load-deflection curves for flanges 20×200 mm, h=200 mm, with a span length of 5000 mm and material 1.4301

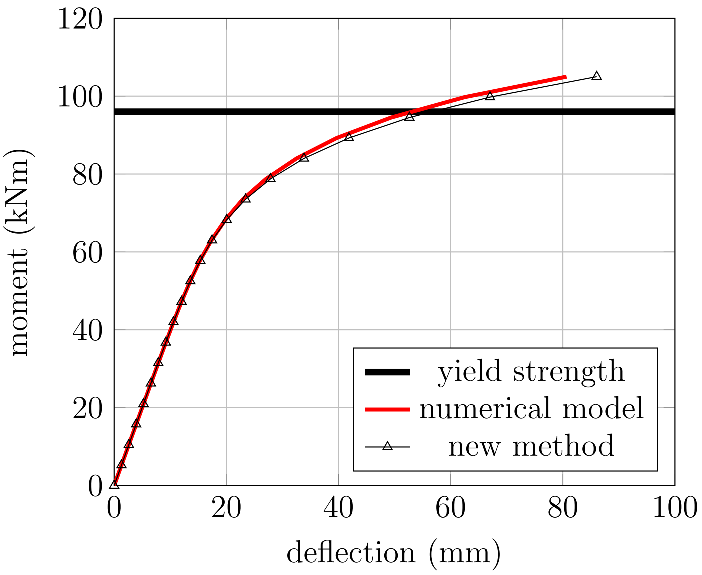

Figure 12: Load-deflection curves for flanges 15×100 mm, h=300 mm, with a span length of 5000 mm and material 1.4301

5.2 Webs

Similarly to sections consisting of flanges in 5.1, numerical models of rectangular sections were made. The value of $E_{ser,w}$ was determined as the value of stress at 1/8 of the height of the web, as shown in Fig. 13. This value can be calculated by (15). However, since the stress distribution is far more varied than at flanges, the results are not as accurate as for the flanges.

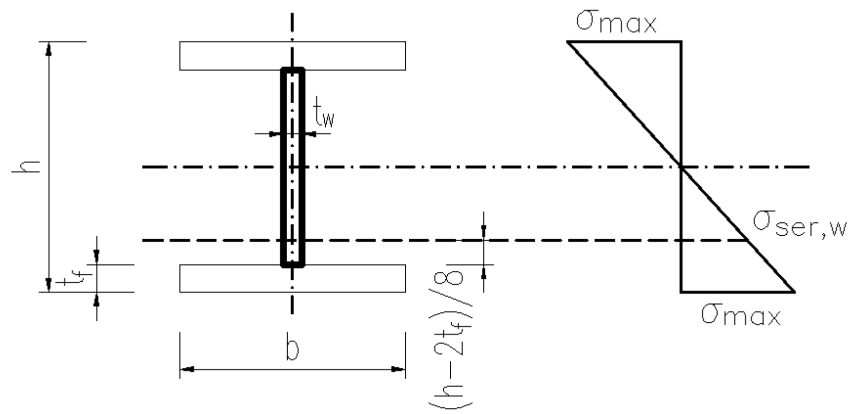

Figure 13: Stress distribution considered for calculation of the secant modulus of web

$$\sigma_{ser,w} = \sigma_{max} \cdot \frac{3(h - 2t_f)}{4h} \tag{15}$$

where $\sigma_{ser,w}$ is the value of stress used for calculation of $E_{secant,w}$ with (4).

Figs. 14 and 15 shows deflections estimated elastically using $E_{secant,w}$ compared to those obtained from the numerical model.

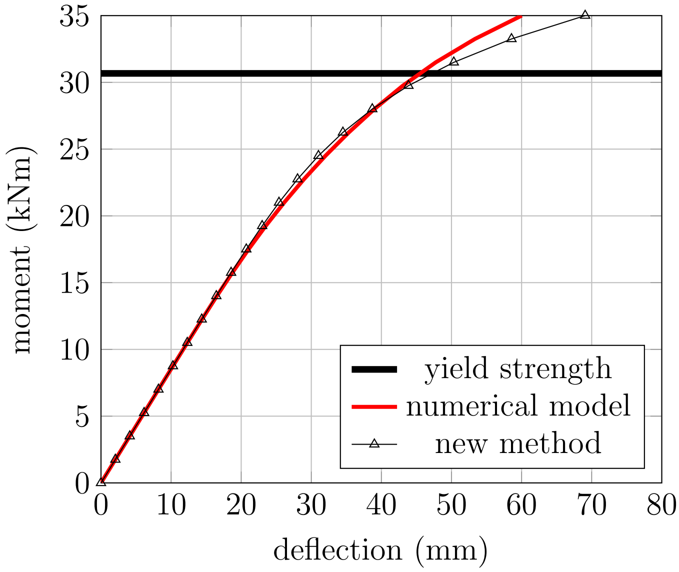

Figure 14: Load-deflection curve for web 20×200 mm with a span length of 5000 mm and material 1.4301

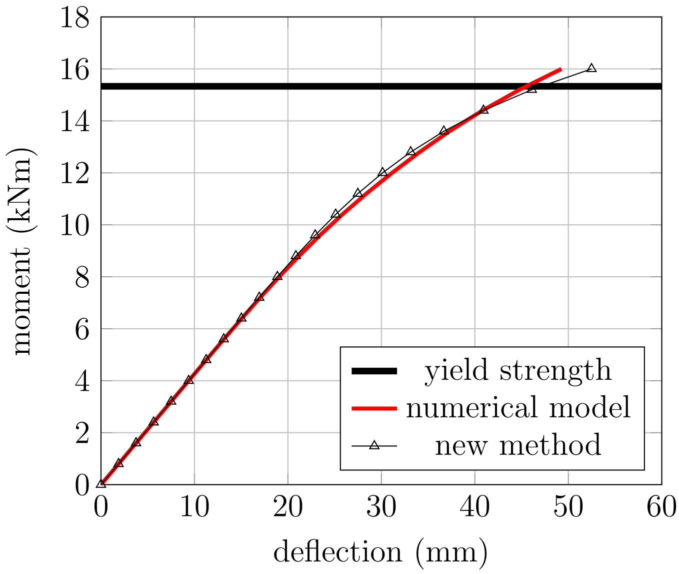

Figure 15: Load-deflection curve for web 10×200 mm with a span length of 5000 mm and material 1.4301

5.3 Simply supported beams

5.3.1 I and RHS cross-sections

In the next step, the stiffness of the cross-section is divided into two parts - the stiffness of flanges and the stiffness of the web. As can be observed in (16), each stiffness is calculated using the corresponding secant modulus.

$$EI = E_{secant,fl} \cdot I_{fl} + E_{secant,w} \cdot I_w \tag{16}$$

where EI is the original stiffness of the full cross-section, $E_{secant,fl}$ and $E_{secant,w}$ are secant moduli of the flanges and of the web, I_{fl} is the moment of inertia of the flanges and I_w is the moment of inertia of the web.

Figs. 16 and 17 show deflections of beams studied in 4.1 calculated using the new method compared to those calculated with other previously mentioned methods. As can be observed, the newly proposed method shows more accurate results than those calculated with Eurocode or R&M method and the results are also not underestimated, unlike those calculated with the R&M-modified method. However, deflections are not as accurate as those delivered by CECS 410 method. Results for all analyzed cross-sections can be seen in Tables 27 and 28 in the Annex. The mean and maximum percentage deviations of deflections are shown in Tabs. 8 and 9. All of the studied beams were made of austenitic steel since it is the most used type of stainless steel and the effect of nonlinearity is the most significant, however, beams made of ferritic and duplex steel were also analyzed. The results for these types of stainless steel can be found in Tables 36 and 37 in the Annex.

Table 8: Mean and maximum deviation of beams subjected to uniform bending moment - I sections

Method	Eurocode	R&M	R&M modified	CECS 410	New method
Mean deviation	17.77 %	23.06 %	-1.35 %	-3.03 %	3.33 %
Maximum deviation	65.39 %	65.39 %	1.61 %	-0.70 %	12.91 %

Table 9: Mean and maximum deviation of beams subjected to uniform bending moment - hollow sections

Method	Eurocode	R&M	R&M modified	New method
Mean deviation	21.41 %	26.77 %	-3.43 %	3.71 %
Maximum deviation	74.30 %	74.30 %	0.22 %	13.68 %

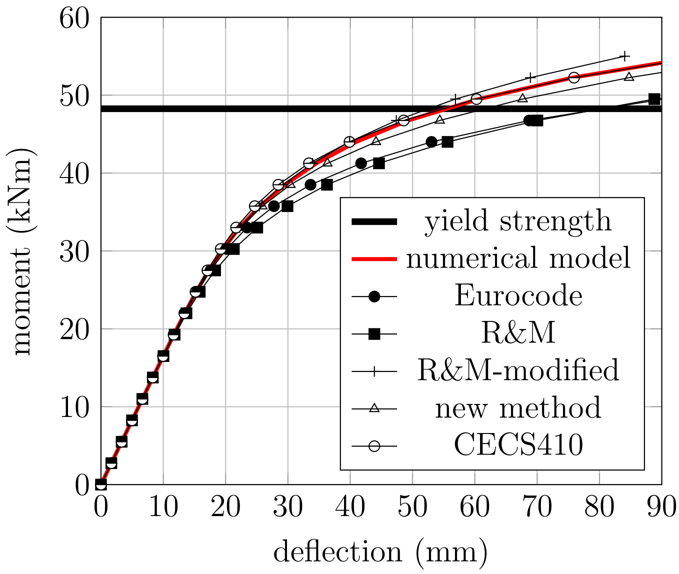

Figure 16: Load-deflection curves for I 200×100 simply supported beam subjected to a uniform bending moment

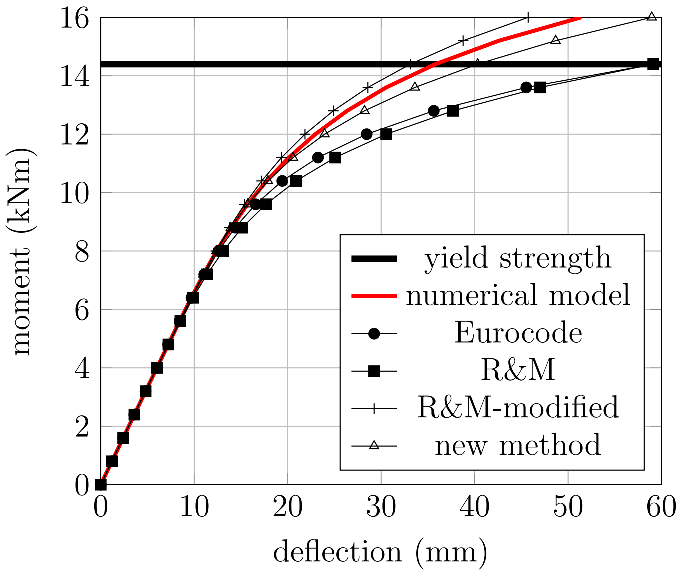

Figure 17: Load-deflection curves for RHS 80×120 simply supported beam subjected to a uniform bending moment

5.3.2 T-sections

Likewise, the new method was applied to T-sections subjected to uniform bending moment and the deflections were compared to those obtained from the numerical model and those calculated by the Eurocode. The properties of analyzed beams are described in Tab. 10. The stress-strain curves are shown in Figs. 20 and 21. Results for all analyzed cross-sections can be found in Tab. 29 in the Annex. The mean and maximum percentage deviations of deflections are shown in Tab. 11.

Table 10: Properties of the studied T-sections

Profile	Total depth h (mm)	Flange width b (mm)	Flange thickness t_f (mm)	Web thickness t_w (mm)	Span length l (mm)	Material
T 200×100	200	100	10	10	5000	1.4301
T 100×100	100	100	10	10	4000	1.4301

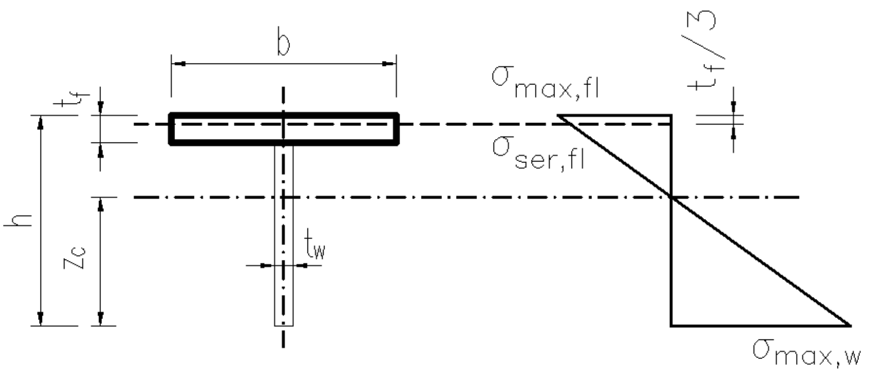

Figure 18: Stress distribution considered for calculation of the secant modulus of the flange for T-sections

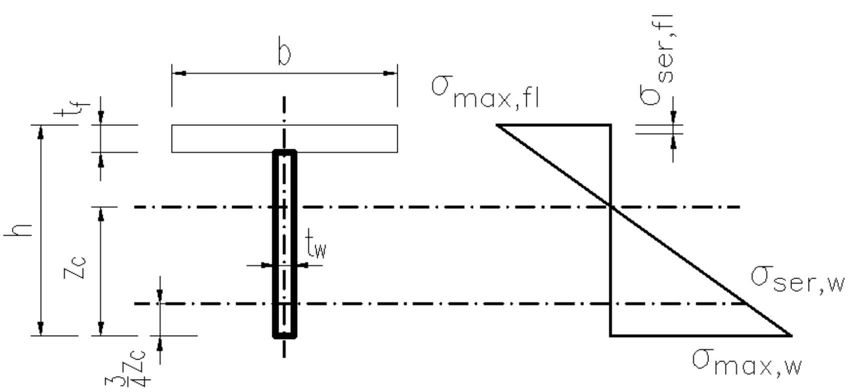

Figure 19: Stress distribution considered for calculation of the secant modulus of the web for T-sections

As can be observed in Fig. 18, the value of stress $\sigma_{ser,fl}$ is calculated by (17) from the maximum stress on the flange $\sigma_{max,fl}$.

$$\sigma_{ser,fl} = \sigma_{max,fl} \cdot \frac{h - z_t}{h - z_t - \frac{t}{3}} \tag{17}$$

The value of stress $\sigma_{ser,w}$ is calculated by (18) from the maximum stress on the web $\sigma_{max,w}$, which is the maximum value of stress on the entire cross-section. Similarly to I cross-sections and hollow sections, $\sigma_{ser,w}$ is considered to be the value of stress at the distance of 3/4 of the height of the web from the neutral axis.

$$\sigma_{ser,w} = \sigma_{max,w} \cdot \frac{3}{4} \tag{18}$$

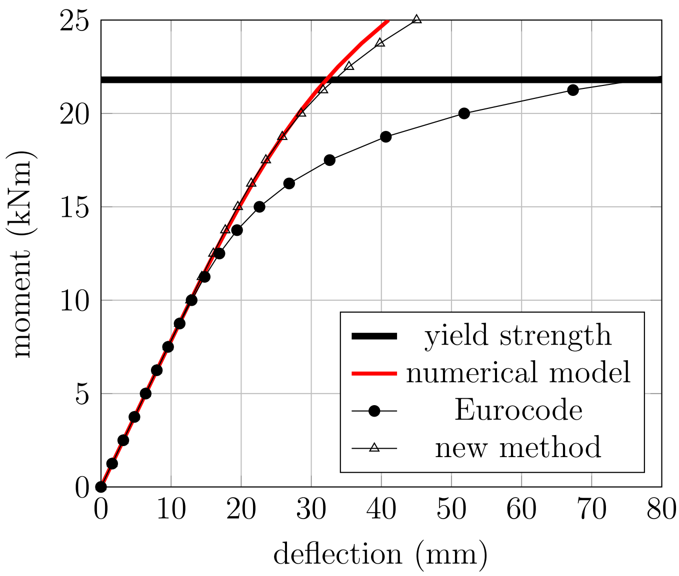

Figure 20: Load-deflection curves for T 200×100 simply supported beam subjected to uniform bending moment

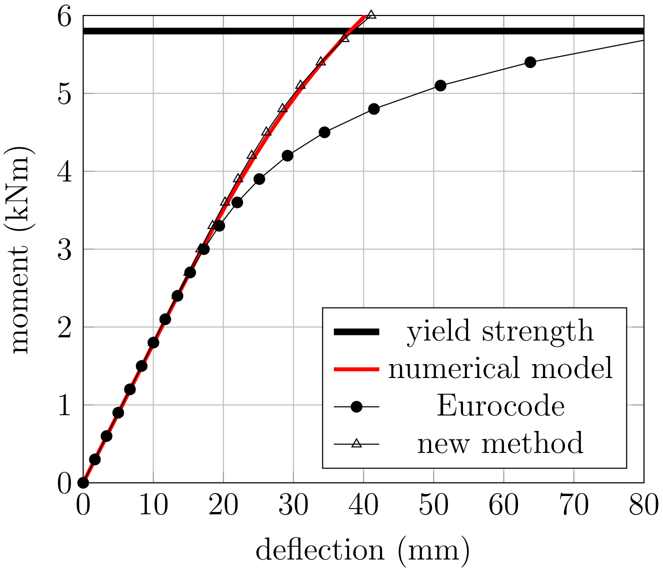

Figure 21: Load-deflection curves for T 100×100 simply supported beam subjected to uniform bending moment

Table 11: Mean and maximum deviation of beams subjected to uniform bending moment - T sections

Method	Eurocode	New method
Mean deviation	44.54 %	0.09 %
Maximum deviation	136.72 %	4.51 %

5.3.3 Asymmetric I cross-sections

Similarly to 5.3.2, the new method was applied to the I cross-section with unequal widths of the top and the bottom flange. Properties of analyzed beams are described in Tab. 12. Since the values of stress in the top and the bottom flange might vary significantly, the most accurate procedure is to determine the secant modulus for each flange separately. The stresses $\sigma_{ser,fl,1}$ and $\sigma_{ser,fl,2}$ are calculated by (19) and described in Fig. 22, whereas the calculation of $\sigma_{ser,w}$ is similar to the case of symmetric I cross-section, calculated by (15). The stiffness of the entire cross-section is then calculated with (20). The stress-strain curves are shown in Figs. 23 and 24. Results for all analyzed cross-sections can be found in Tab. 30 in the Annex. The mean and maximum percentage deviations of deflections are shown in Tab. 13.

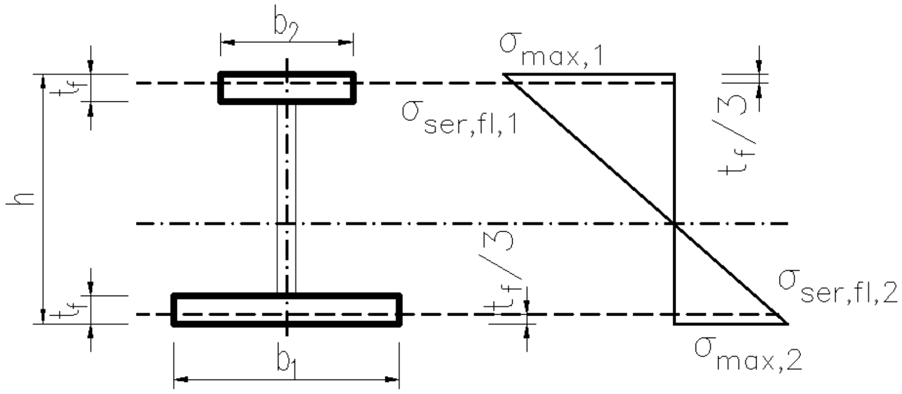

Figure 22: Stress distribution considered for calculation of the secant modulus of the web for asymmetric I cross-sections

$$\sigma_{ser,fl,i} = \sigma_{max,i} \cdot \frac{h - \frac{2}{3}t_f}{h} \tag{19}$$

where $\sigma_{max,i}$ is the value of stress at the extreme fibers of flange 1 and flange 2.

$$EI = E_{secant,fl,1}I_{fl,1} + E_{secant,fl,2}I_{fl,2} + E_{secant,w}I_w \tag{20}$$

where $E_{secant,fl,1}$ is the secant modulus of flange 1, $E_{secant,fl,2}$ is the secant modulus of flange 2, $I_{fl,1}$ is the moment of inertia of flange 1 and $I_{fl,2}$ is the moment of inertia of flange 2.

Table 12: Properties of studied asymmetric I cross-sections

Profile	Total depth h (mm)	Flange width 1 b_1 (mm)	Flange width 2 b_2 (mm)	Flange thickness t_f (mm)	Web thickness t_w (mm)	Span length l (mm)	Material
I 200	200	200	100	20	10	6000	1.4301
I 300	300	300	100	20	10	6000	1.4301

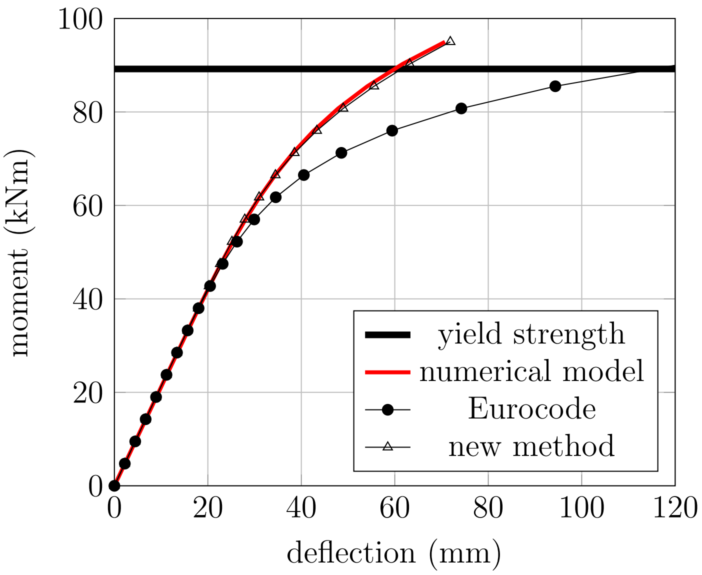

Figure 23: Load-deflection curves for I 200 simply supported beam subjected to uniform bending moment

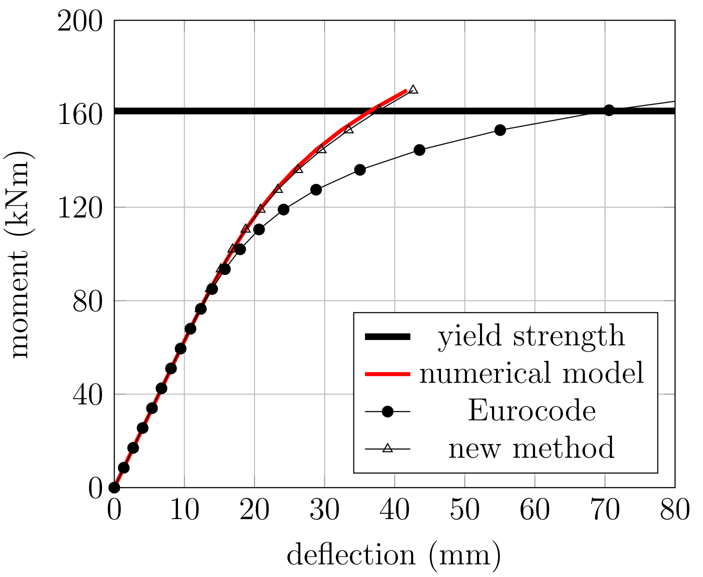

Figure 24: Load-deflection curves for I 300 simply supported beam subjected to uniform bending moment

Table 13: Mean and maximum deviation of beams subjected to uniform bending moment - asymmetrical I sections

Method	Eurocode	New method
Mean deviation	32.22 %	1.46 %
Maximum deviation	99.48 %	5.97 %

5.4 Non-uniform bending moment

The results for a uniform bending moment are satisfying, however, the deflections are very conservative for a non-uniform bending moment, since the method does not take into account the variation of stress along the beam length. Therefore, a coefficient k to reduce the stresses $\sigma_{ser,fl}$ and $\sigma_{ser,w}$ is applied for different load cases.

The procedure of determining these coefficients is presented on an example of a simply supported beam subjected to a concentrated load at mid-span. At first, two models of the same beam were made. One was loaded by a uniform bending moment that corresponds to the maximum moment of resistance of the cross-section and the other one was subjected to a concentrated load at mid-span, which causes the same bending moment. Now, two deflections are obtained from these models. From these deflections, secant moduli, which lead to these deflections, can be calculated with (21) and (22). These equations originated by expressing the modulus of elasticity from basic linear equations used for the determination of deflections of simply supported beams.

For beam subjected to a uniform bending moment:

$$E_{secant,1} = \frac{ML^2}{8Id_1} \tag{21}$$

For beam subjected to a concentrated load at mid-span:

$$E_{secant,2} = \frac{ML^3}{48Id_2} \tag{22}$$

where d_1 and d_2 are deflections obtained from numerical models.

Furthermore, corresponding stress values are calculated with (23), which originated by expressing σ_{ser} from (4).

$$\sigma_i = \sqrt[n-1]{\frac{f_y^n \left(\frac{E_0}{E_{secant,i}} - 1\right)}{0.002E_0}} \tag{23}$$

Finally, the coefficient is a ratio of these values calculated with:

$$k = \frac{\sigma_2}{\sigma_1} \tag{24}$$

where k is the desired coefficient, σ_2 is the value of stress obtained by using (22) and (23) and σ_1 is the value of stress obtained by using (21) and (23).

The deflections of simply supported beams are then calculated linearly, using the secant modulus given by (25). This procedure is similar for all load cases.

$$E_{secant} = \frac{E_0}{1 + 0.002\,\frac{E_0}{k \cdot \sigma_{ser}}\left(\frac{k\sigma_{ser}}{f_y}\right)^n} \tag{25}$$

Figs. 25 and 26 show results for beams subjected to a concentrated load at mid-span calculated with the newly proposed method using coefficient k compared to those delivered by other methods.

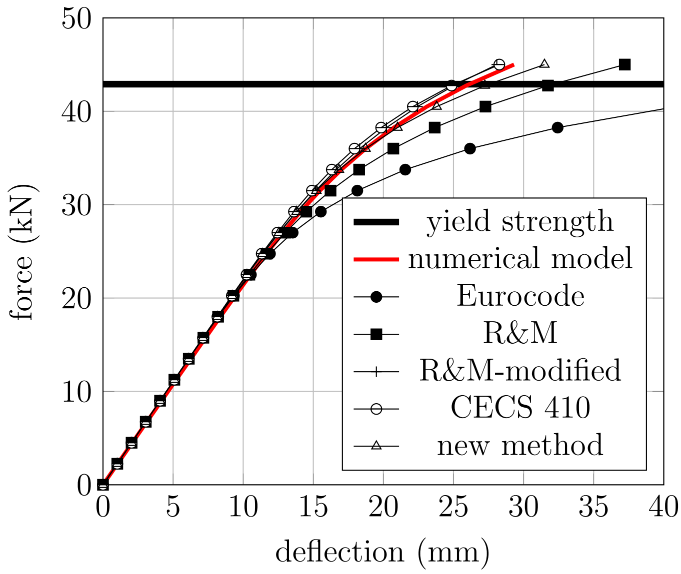

Figure 25: Load-deflection curves for I 200×100 simply supported beam subjected to a concentrated load at mid-span

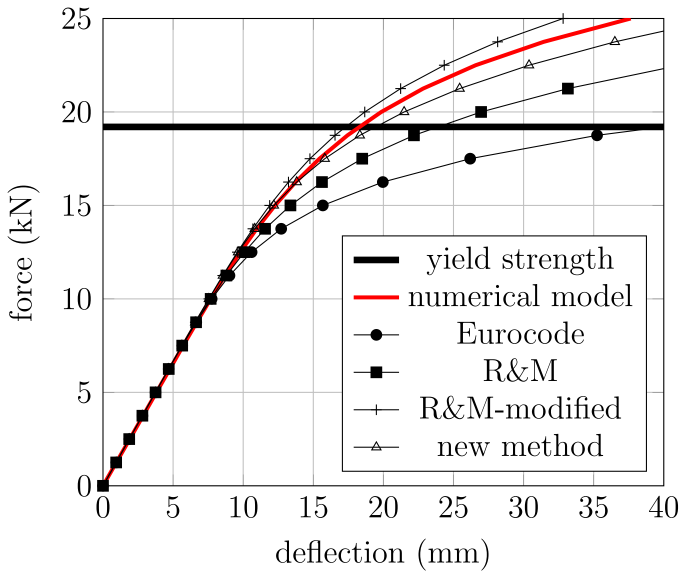

Figure 26: Load-deflection curves for RHS 80×120 simply supported beam subjected to a concentrated load at mid-span

Similarly to the case of a beam loaded by a concentrated load at mid-span, the coefficients for the cases of uniformly distributed load and two concentrated loads at thirds of the span length were found. Tabs. 14 to 16 show the mean and maximum percentage deviations of deflections of simply supported beams subjected to these basic load cases. The deflections of all tested beams can be found in Tables 31 to 35 in the Annex.

Table 14: Mean and maximum deviation of beams subjected to concentrated load at mid-span

Method	Eurocode	R&M	R&M modified	CECS 410	New method
Mean deviation	37.03 %	9.80 %	-2.29 %	-3.31 %	0.40 %
Maximum deviation	121.32 %	33.49 %	-0.58 %	-1.75 %	7.00 %

Table 15: Mean and maximum deviation of beams subjected to uniformly distributed load

Method	Eurocode	R&M	R&M modified	CECS 410	New method
Mean deviation	27.68 %	16.74 %	-2.38 %	-3.32 %	2.23 %
Maximum deviation	96.12 %	53.16 %	-0.08 %	-1.62 %	11.41 %

Table 16: Mean and maximum deviation of beams subjected to two concentrated loads at thirds of the span

Method	Eurocode	New method
Mean deviation	26.54 %	1.04 %
Maximum deviation	90.93 %	11.45 %

In the next step, beams with linear moment distribution were studied. Models of simply supported beams were subjected to two non-equal support moments. The loading scheme and moment distribution are shown in Fig. 27.

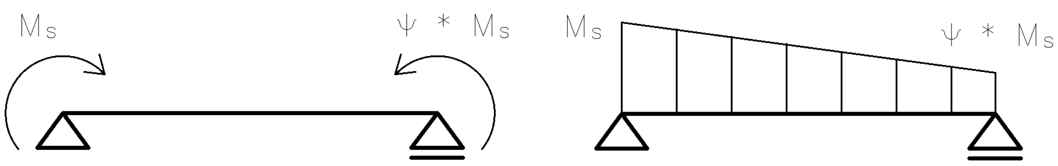

Figure 27: Linear moment distribution and load scheme

Table 17: coefficient k depending on the support bending moments ratio ψ

ψ	-1	-0.75	-0.5	-0.25	0	0.25	0.5	0.75	1
k	0.72	0.72	0.72	0.72	0.72	0.75	0.81	0.89	1.00

Tab. 17 shows calculated values of coefficient k for the range of ψ from -1 to 1. The value of k is constant for the range of ψ from -1 to 0 (26). For the range from 0 to 1, an equation (27) for the calculation of the coefficient k was found, using the trend connection function in MS Excel.

for $-1 \leq \psi \leq 0$:

$$k = 0.72 \tag{26}$$

for $0 \leq \psi \leq 1$:

$$k = 0.2\psi^2 + 0.07\psi + 0.72 \tag{27}$$

Likewise, beams with parabolic moment distribution were analyzed by applying a uniformly distributed load on simply supported beams with non-equal support moments. The load scheme and moment distribution are shown in Fig. 28.

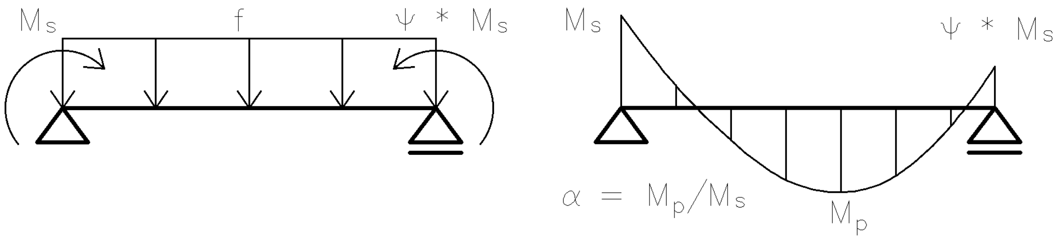

Figure 28: Parabolic moment distribution and load scheme

Table 18: coefficient k depending on ψ and α

ψ / α	0	0.25	0.5	0.75	1
-2	0.93	0.93	0.93	0.93	0.93
-1.5	0.93	0.93	0.93	0.93	0.93
-1	0.93	0.93	0.93	0.93	0.93
-0.75	0.73	0.73	0.73	0.73	0.73
-0.5	0.61	0.63	0.65	0.66	0.67
0.25	-	-	0.55	0.47	0.51
0.5	-	-	-	0.64	0.65
0.75	-	-	-	-	0.85

Tab. 18 shows values of k depending on the values of ψ and α. It can be observed, that when a distributed load is applied, the value of k does not change significantly with the change of ψ. Therefore, this change can be neglected and it is assumed, that the value of k depends only on the change of α. Using the same procedure as described above, relationships for calculating k were found. Equations (28) and (29) describe the relationship between k and α for negative and positive values of α.

Furthermore, it is true that when α is in the range from -0.5 to 0.5, the reduction coefficient k reaches the point, when the deviation between calculated deflection and linear deflection is not higher than 5 % and therefore the material non-linearity can be neglected.

for $\alpha \leq -0.5$:

$$k = 0.6\alpha^2 + 0.27\alpha + 0.6 \ \leq 0.93 \tag{28}$$

for $\alpha \geq 0.5$:

$$k = 0.75\alpha + 0.25 \tag{29}$$

Tab. 19 shows values of coefficient k for studied loading cases.

Table 19: Values of coefficient k for various load cases

Load case		k
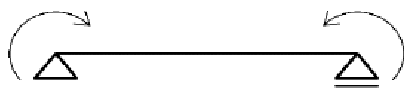		1.00
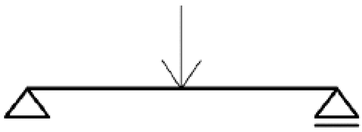		0.84
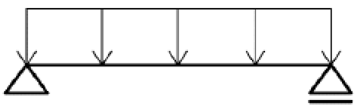		0.93
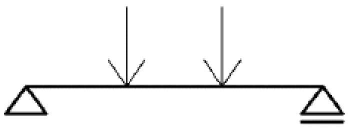		0.95
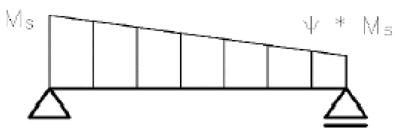	$-1 \leq \psi \leq 0$	0.72
	$0 \leq \psi \leq 1$	$0.2\psi^2 + 0.07\psi + 0.72$
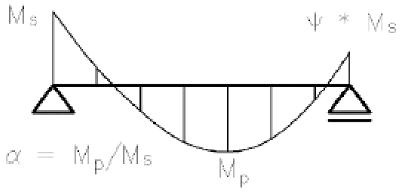	$\alpha \leq -0.5$	$0.6\alpha^2 + 0.27\alpha + 0.6 \leq 0.93$
	$\alpha \leq 0.5$	$0.75\alpha + 0.25$

5.5 Portal frames

Since the new method was extended to beams with the general distribution of the bending moment, it can be also applied to portal frames. Below, frames subjected to horizontal forces and vertical distributed load were analyzed. Similarly to braced portal frames 4.2, deflections obtained from numerical models were compared to those calculated by linear analysis. **Linear deflection** and **Eurocode deflection** were calculated similarly to those in 4.2. These deflections were compared with each other and also with the deflection calculated by the new method (**New method deflection**).

When using the new method, the secant modulus was calculated separately for each member of the frame. The secant moduli were calculated separately for flanges and webs of the cross-sections, as described in 5.1 and 5.2. Since all members of the frame are subjected to non-uniform bending moment, the stresses used for calculation of the secant modulus ($\sigma_{ser,fl}$, $\sigma_{ser,w}$) were reduced by corresponding coefficient k. The value of the coefficient was determined separately for each member of the frame, based on the distribution of the bending moment, according to Tab. 19.

However, since the members in the Dlubal RFEM5 software can not be split into webs and flanges (therefore, two different secant moduli can not be applied for one member), a mean value of the secant modulus must be determined by (30).

$$E_{ser} = \frac{E_{ser,fl} \cdot I_{fl} + E_{ser,w} \cdot I_w}{I} \tag{30}$$

where I is the moment of inertia of the entire cross-section.

5.5.1 Frames subjected to horizontal loads

Three portal frames with pinned supports and three portal frames with rigid supports were subjected to horizontal forces at the tops of the columns according to Fig. 29. All frames are made of cross-section HEA 200 and material 1.4301. The geometry of the frames is described in Tab. 20.

Table 20: Geometry of analyzed portal frames

Frame	Span length L (m)	Height H (m)
Fr. 1	4	2
Fr. 2	2	4
Fr. 3	6	2

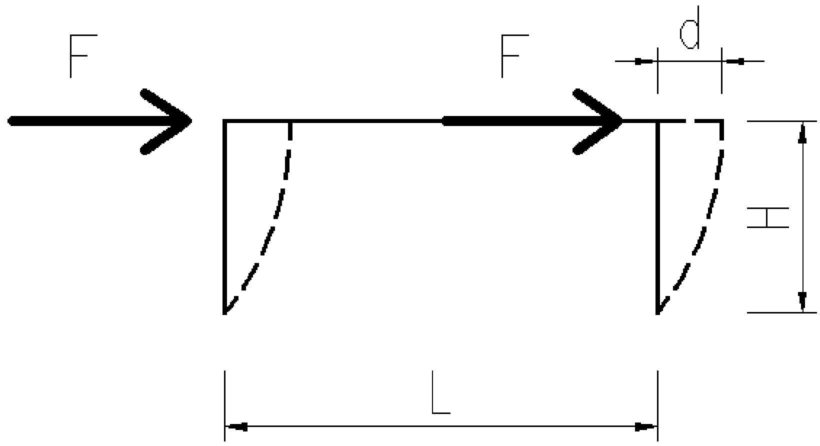

Figure 29: Load scheme of portal frames subjected to horizontal forces

The results are shown in Tabs. 21 and 22. for load steps corresponding to 60 %, 80 % and 100 % of the magnitude of loading forces, where 100 % of the force magnitude leads to maximum stress on the structure equal to the yield strength.

Table 21: Horizontal deflections of portal frames with pinned supports

Frame	Load step	Force (kN)	Elastic defl. (mm)	Abaqus defl. (mm)	Eurocode defl. (mm)	New method defl. (mm)
Fr. 1	60 %	45.6	19.23	18.76	20.79	19.36
	80 %	60.8	25.64	26.29	37.32	26.66
	100 %	76.0	32.05	37.86	87.78	36.91
Fr. 2	60 %	22.0	47.00	45.87	49.54	47.22
	80 %	29.4	62.81	64.02	81.92	64.49
	100 %	36.7	78.4	90.98	214.76	90.30
Fr. 3	60 %	46.2	23.71	23.50	25.63	23.88
	80 %	61.6	31.61	33.06	46.03	32.88
	100 %	77.0	39.52	48.05	108.25	45.51

Table 22: Horizontal deflections of portal frames with rigid supports

Frame	Load step	Force (kN)	Elastic defl. (mm)	Abaqus defl. (mm)	Eurocode defl. (mm)	New method defl. (mm)
Fr. 1	60 %	73.2	7.55	6.87	8.16	7.58
	80 %	97.6	10.06	9.41	14.65	10.35
	100 %	122.0	12.58	12.57	34.44	13.94
Fr. 2	60 %	40.5	22.00	20.95	23.78	22.12
	80 %	54.0	29.33	28.80	42.70	30.28
	100 %	67.5	36.66	39.24	100.42	41.37
Fr. 3	60 %	69.6	7.94	7.36	8.59	7.98
	80 %	92.8	10.59	10.11	15.42	10.89
	100 %	116.0	13.24	13.55	36.27	14.65

It can be observed, that the effect of non-linearity should be taken into account for portal frames, in which the maximum stress exceeds approximately 80 % of yield strength. Furthermore, the difference between **Elastic deflection** and **Abaqus deflection** is more significant for higher frames with lower span length, whereas this difference is lower or even none for lower frames with larger spans. Moreover, the non-linearity has almost no impact on frames with rigid supports.

Deflections calculated by the method provided in the Eurocode are generally significantly overestimated, whereas those calculated with the new method are more accurate, however, sometimes underestimated. Nevertheless, the underestimation is not higher than 5 %.

5.5.2 Frames subjected to vertical distributed load

Portal frames from 5.5.1 were subjected to vertical distributed load according to Fig. 30. The results are shown in Tabs. 23 and 24.

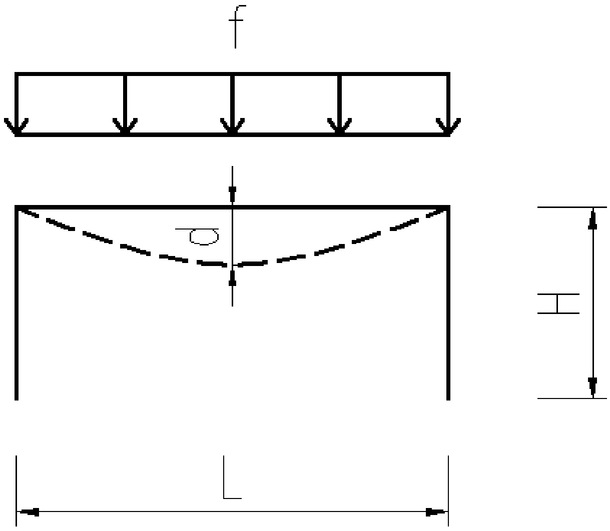

Figure 30: Load scheme of portal frames subjected to vertical distributed load

Table 23: Vertical deflections of portal frames with pinned supports

Frame	Load step	Load (kN/m)	Elastic defl. (mm)	Abaqus defl. (mm)	Eurocode defl. (mm)	New method defl. (mm)
Fr. 1	60 %	92.7	10.95	10.22	11.84	11.19
	80 %	123.6	14.60	14.87	21.25	16.51
	100 %	154.5	18.24	23.22	49.98	25.11
Fr. 2	60 %	264.0	4.23	3.68	4.58	4.33
	80 %	352.0	5.65	5.16	8.22	6.34
	100 %	440.0	7.06	7.17	19.33	9.58
Fr. 3	60 %	39.1	18.63	17.96	20.15	18.82
	80 %	52.2	24.88	25.39	36.22	26.55
	100 %	65.2	31.07	37.30	85.11	38.96

Table 24: Vertical deflections of portal frames with rigid supports

Frame	Load step	Load (kN/m)	Elastic defl. (mm)	Abaqus defl. (mm)	Eurocode defl. (mm)	New method defl. (mm)
Fr. 1	60 %	92.8	10.42	9.46	11.27	10.64
	80 %	123.7	13.89	13.67	20.23	15.48
	100 %	154.6	17.37	21.10	47.57	24.72
Fr. 2	60 %	279.6	4.27	3.66	4.62	4.37
	80 %	372.8	5.7	5.11	8.30	6.38
	100 %	466.0	7.12	7.09	19.51	10.13
Fr. 3	60 %	38.1	17.29	16.26	18.69	17.46
	80 %	50.8	23.05	22.79	33.56	24.29
	100 %	63.5	28.82	32.67	78.93	34.66

When analyzing vertical deflections, the effect of non-linearity only becomes apparent when the maximum stress exceeds 85 - 90 % of the yield strength and it is also only significant for frames with larger spans. Similarly to 5.5.1, deflections calculated by the method provided in Eurocode are highly overestimated, whereas the new method gives deflections that are very close to those obtained from the numerical model.

5.6 Trusses

Three trusses subjected to vertical load were analyzed in the Abaqus code. Obtained vertical deflections at mid-span were compared to those calculated by linear analysis, using Dlubal RFEM5 software. Similarly to braced portal frames 4.2, three different deflections for each truss were obtained from this software (**linear deflection** - using the initial Young's modulus E_0, **Eurocode deflection** - using the same secant modulus for the entire structure, calculated (4), σ_{ser} is the maximum magnitude of stress on the structure and **New method deflection** - applying the secant modulus only to the flanges of the truss and reducing the σ_{ser} with coefficient k, which equals to 0.93 for this type of load (uniformly distributed load, concentrated to the nodes of the truss) according to Fig. 31.

In all models, the cross-sections are set so the stress in the top flange is equal to the yield strength. Furthermore, in each truss, the diagonals are made of two types of cross-sections (inner diagonals and outer diagonals), both adjusted so that the stress in the most loaded member is equal to the yield strength. All members are made of CHS cross-sections. The geometry and cross-sections are described in Tab. 25. The stress distribution is shown in Fig. 32. The material used for all trusses is 1.4301.

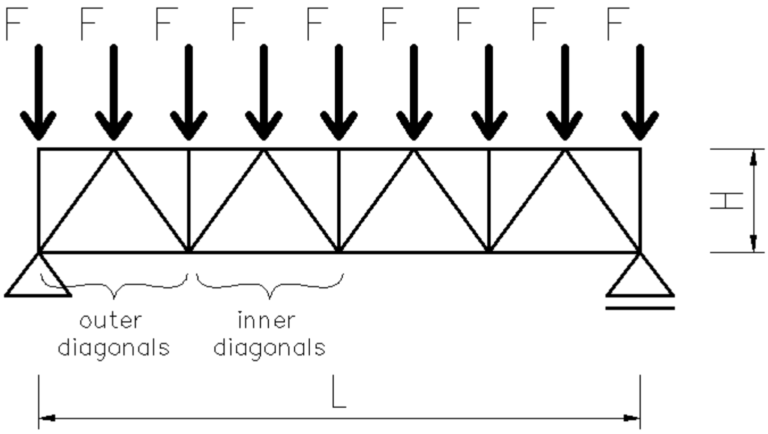

Figure 31: Loading scheme of analyzed trusses

Table 25: Description of geometry and cross-sections of analyzed trusses

Truss	Span length L (m)	Heigth H (m)	Flanges	Outer diagonals	Inner diagonals	Verticals
Tr. 1	20	2.0	150/6	70/6.5	50/4	50/4
Tr. 2	30	2.6	150/6	70/5.3	60/3.9	60/3.9
Tr. 3	60	3.5	330/20	160/10.5	100/10	100/10

σ [MPa]:

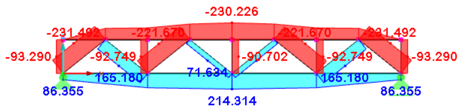

(a) Truss Tr. 1

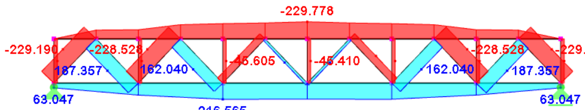

(b) Truss Tr. 2

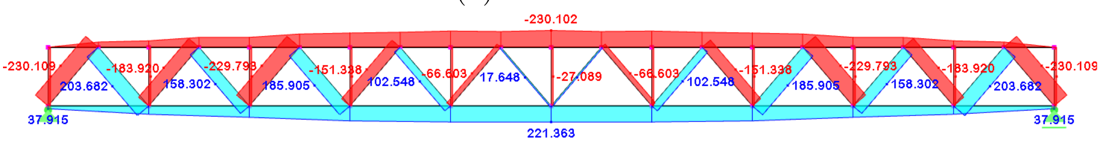

(c) Truss Tr. 3

Figure 32: Stress distribution for analyzed trusses subjected to 100 % of loading forces

Table 26: Vertical deflections of analyzed trusses

Truss	Load step	Force (kN)	Elastic defl. (mm)	Abaqus defl. (mm)	Eurocode defl. (mm)	New method defl. (mm)
Tr. 1	60 %	32.2	36.3	36.84	39.25	37.61
	80 %	43.0	48.48	55.84	70.58	58.41
	100 %	53.7	60.54	97.04	174.48	113.65
Tr. 2	60 %	19.4	59.9	61.05	64.32	61.83
	80 %	25.9	79.43	92.88	115.64	97.16
	100 %	32.4	99.36	162.99	272.16	184.33
Tr. 3	60 %	54.6	156.97	161.05	169.70	163.64
	80 %	72.8	209.29	238.92	304.71	259.85
	100 %	91.0	261.61	395.59	716.60	503.67

Similarly to simply supported beams and braced portal frames, the effect of non-linearity should be taken into account for trusses, in which the maximum stress exceeds approximately 50 % of the yield strength. Deflections calculated by the new method are much closer to the actual deflections than those calculated by the method provided in Eurocode.

6 Conclusion

In this thesis, deflections of stainless steel structures were studied. Deflections of simply supported beams calculated using several methods were compared to those obtained from validated numerical models. The current design method provided in the Eurocode was verified on every studied structure. Then, a new method for calculating deflections was proposed.

Simply supported beams subjected to basic load cases were analyzed. The deflections were calculated by the method stated in the Eurocode, a method provided by Real and Mirambell [7] (using two different moments of resistance, explained in 2.3) and a method provided in the Chinese code [1]. The two methods, that provide the most accurate results are the method proposed by Real and Mirambell with the usage of a modified moment of resistance and the method provided in the Chinese code, however, the deflections might sometimes be slightly underestimated. Another conclusion is that the effect of non-linearity can be neglected for beams, in which the maximum stress does not exceed 50 % of the yield stress.

Furthermore, braced portal frames subjected to horizontal forces were tested in 4.2. Deflections obtained from the numerical models were compared to those calculated with linear analysis, using Dlubal RFEM5 software. When using the method provided in the Eurocode (calculating the secant modulus from the maximum stress and applying it on the entire structure), the obtained deflections are sufficient, however, they may be overestimated. Therefore, a new procedure was proposed, in which the secant modulus is calculated separately for the frame and for the bracings, using the maximum stress on each part. This method gives the most accurate results. Similarly to simply supported beams, the effect of non-linearity should be only taken into account when the maximum stress on the structure exceeds 50 % of the yield stress.

In chapter 5 of the thesis, a new method for calculating deflections of simply supported beams was proposed. The main motivation behind this proposal was the fact, that the existing methods (Real and Mirambell, CECS 410) can only be used for a few basic loading cases and the calculation procedure is lengthy and complicated. The newly proposed method consists of dividing the cross-section into webs and flanges and calculating and applying the secant modulus of elasticity on each part separately. The variation of Young's modulus along the length of the beam is then taken into account by the application of a coefficient, whose values were calculated for basic load cases (uniform bending moment, concentrated load at mid-span, uniformly distributed load, two concentrated loads at thirds of the span). Furthermore, equations for calculating the coefficient for linear and parabolic distribution of bending moment were created in 5.4. The values of the coefficient for studied load cases are shown in Tab. 19.

The deflections calculated with the newly proposed method are very accurate, although they might be slightly overestimated for values of stress close to the yield strength. One of the main advantages of this method is the fact, that it can be also used for estimating the deflection of portal frames, as described in 5.5. When calculating the deflections of portal frames by the method provided in the Eurocode, the deflections are highly overestimated, therefore, a more accurate method is very useful. The new method is applied by calculating the secant modulus separately for each member, using the same method as for simply supported beams in 5.3, and applying the reducing coefficient for a non-uniform bending moment. The effect of non-linearity should be taken into account for portal frames, in which the maximum stress exceeds approximately 80 % of the yield stress.

Finally, three trusses with different span lengths were studied in 5.6. Similarly to simply supported beams and braced portal frames, the effect of non-linearity should be taken into account for trusses, in which the maximum stress exceeds approximately 50 % of the yield strength. Since the deflections calculated by the method provided in the Eurocode are highly overestimated, a new procedure was proposed. When using the newly proposed procedure, the secant modulus is applied only for the flanges, whereas Young's modulus of the diagonal and vertical members is considered equal to the initial modulus of elasticity E_0. Moreover, when calculating the secant modulus of the flanges, the reducing coefficient from Tab. 19 is applied. The deflections calculated with the new procedure are very close to those obtained from the numerical model.

7 Example

Below, an example of the application of the newly proposed method is presented by estimating a deflection of a simply supported beam subjected to a uniformly distributed load.

Asignment

simply supported beam subjected to uniformly distributed load
span length (l): $6\,m$
load (f): $10\,kN/m$
cross-section: I 200 ($W_y = 2.10 \times 10^5\,mm^3$, $h = 200\,mm$, $b = 100\,mm$, $t_f = 10\,mm$, $t_w = 6\,mm$)
material: 1.4301 ($E_0 = 200000\,MPa$, $f_y = 230\,MPa$, $n = 7$)

Solution

1. Determination of maximum stress

Using basic structural mechanics, the maximum bending moment (M_{max}) and then the maximum stress (σ_{max}) is determined.

$$M_{max} = \frac{fl^2}{8} = \frac{10 \cdot 6^2}{8} = 36\,kNm$$

$$\sigma_{max} = \frac{M}{W_y} = \frac{36 \times 10^6}{2.1 \times 10^5} = 194.59\,MPa$$

2. Determination of secant moduli of elasticity

Using (14) and (15), the values of stress $\sigma_{ser,fl}$ and $\sigma_{ser,w}$ are determined.

$$\sigma_{ser,fl} = \sigma_{max} \cdot \frac{h - \frac{2}{3} \cdot t_f}{h} = 194.59 \cdot \frac{200 - \frac{2}{3} \cdot 10}{200} = 188.10\,MPa$$

$$\sigma_{ser,w} = \sigma_{max} \cdot \frac{3(h - 2t_f)}{4h} = 194.59 \cdot \frac{3 \cdot (200 - 2 \cdot 10)}{4 \cdot 200} = 131.35\,MPa$$

Then, a coefficient k is picked from Tab. 19 for a simply supported beam with uniformly distributed load:

$$k = 0.93$$

Using (25), secant moduli $E_{ser,fl}$ and $E_{ser,w}$ are determined.

$$E_{secant,fl} = \frac{E_0}{1 + 0.002\,\frac{E_0}{k \cdot \sigma_{ser}}\left(\frac{k \cdot \sigma_{ser}}{f_y}\right)^n} = \frac{200000}{1 + 0.002 \cdot \frac{200000}{0.93 \cdot 188.10}\left(\frac{0.93 \cdot 188.10}{230}\right)^7} =$$

$$= 149626.3\,MPa$$

$$E_{secant,w} = \frac{E_0}{1 + 0.002\,\frac{E_0}{k \cdot \sigma_{ser}}\left(\frac{k \cdot \sigma_{ser}}{f_y}\right)^n} = \frac{200000}{1 + 0.002 \cdot \frac{200000}{0.93 \cdot 131.35}\left(\frac{0.93 \cdot 131.35}{230}\right)^7} =$$

$$= 192486.5\,MPa$$

3. Determination of moments of inertia

Moments of inertia of the flanges and the web must be calculated.

$$I_{fl} = 2 \cdot \left(\frac{b \cdot t_f^3}{12} + b \cdot t_f \cdot \left(\frac{h}{2} - \frac{t_f}{2}\right)^2\right) =$$

$$= 2 \cdot \left(\frac{100 \cdot 10^3}{12} + 100 \cdot 10 \cdot \left(\frac{200}{2} - \frac{10}{2}\right)^2\right) = 1.81 \times 10^7\,mm^4$$

$$I_w = \frac{t_w \cdot (h - 2 \cdot t_f)^3}{12} = \frac{6 \cdot (200 - 2 \cdot 10)^3}{12} = 2.92 \times 10^6\,mm^4$$

Determination of deflection

The deflection of the beam is determined by basic formula for calculating the deflection of simply supported beams subjected to uniformly distributed load, with the stiffness EI replaced by $E_{secant,fl} \cdot I_{fl} + E_{secant,w} \cdot I_w$, as shown in (16).

$$d = \frac{5 \cdot f \cdot l^4}{384 \cdot (E_{secant,fl} \cdot I_{fl} + E_{secant,w} \cdot I_w)} =$$

$$= \frac{5 \cdot 10 \cdot 6000^4}{384 \cdot (149626.3 \cdot 1.81 \times 10^7 + 192486.5 \cdot 2.92 \times 10^6)} = 60.30\,mm$$

8 References

[1] CECS 410: 2015. *Technical specification for stainless steel structures*. Beijing: China Planning Press, 2015.

[2] Version Abaqus. 6.14 documentation. *Dassault Systemes Simulia Corporation*, 651(6.2), 2014.

[3] S Afshan, O Zhao, and L Gardner. Standardised material properties for numerical parametric studies of stainless steel structures and buckling curves for tubular columns. *Journal of Constructional Steel Research*, 152:2–11, 2019.

[4] Eurocode EC. *3: Design of steel structures Part 1.4: General rules—supplementary rules for stainless steels, European Committee for Standardization*. EN 1993-1-4, CEN, Brussels, 2006.

[5] YUAN Huan-xin, CHEN Xiao-wan, CAI Ji-sheng, and DU Xin-xi. Non-linear deflection performance of welded stainless steel i-section beams. , 38(1):78–88, 2021.

[6] Enrique Mirambell and EJJoCSR Real. On the calculation of deflections in structural stainless steel beams: an experimental and numerical investigation. *Journal of Constructional Steel Research*, 54(1):109–133, 2000.

[7] E Real and E Mirambell. Flexural behaviour of stainless steel beams. *Engineering Structures*, 27(10):1465–1475, 2005.

[8] SCI. *Design Manual for Structural Stainless Steel 4th Edition - Commentary*, 2017.

9 Annex

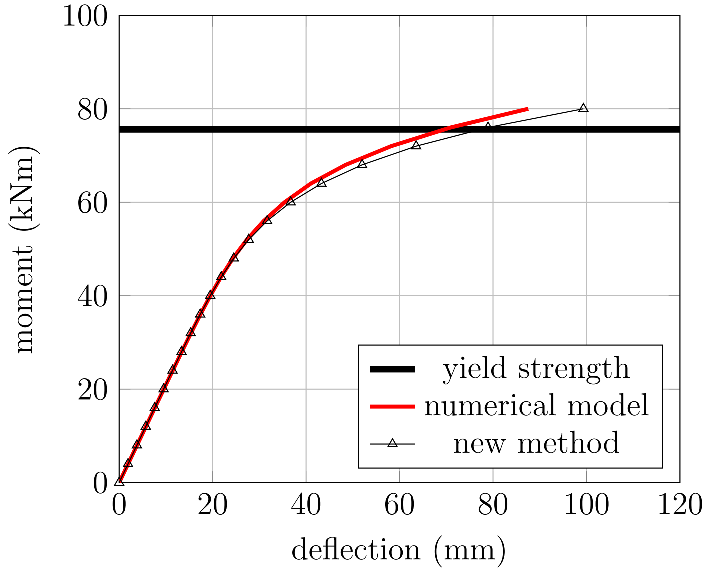

Figure 33: Load-deflection curves for flanges 20×100 mm, h=200 mm, with a span length of 5000 mm and material 1.4301

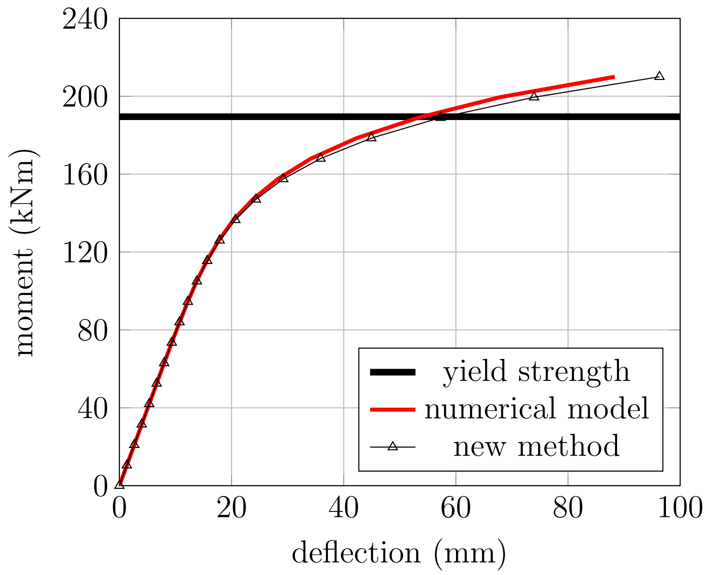

Figure 34: Load-deflection curves for flanges 15×200 mm, h=300 mm, with a span length of 5000 mm and material 1.4301

Table 27: Deflection of simply supported beams subjected to uniform bending moment - I sections[4](1.4301)

Load step	Elastic defl. (mm)	Abaqus (mm)	Eurocode (mm)	R&M (mm)	R&M mod. (mm)	CECS 410 (mm)	New method (mm)
I 100/50/6/4, $l = 3000\,mm$							
50 %	12.94	13.21	13.29	13.64	13.23	13.10	13.18
60 %	15.53	16.37	16.78	17.62	16.39	16.10	16.38
70 %	18.11	20.39	21.82	23.41	20.30	19.81	20.59
80 %	20.70	26.04	30.14	32.50	25.58	25.02	26.88
90 %	23.29	34.34	44.81	47.20	33.17	33.15	36.89
100 %	25.88	47.31	70.88	70.88	44.48	46.49	52.87
I 300/100/15/6, $l = 6000\,mm$							
50 %	17.25	17.62	17.72	18.19	17.68	17.49	17.58
60 %	20.70	21.86	22.38	23.50	21.98	21.54	21.89
70 %	24.15	27.39	29.09	31.21	27.39	26.64	27.63
80 %	27.60	35.20	40.18	43.33	34.81	33.93	36.28
90 %	31.05	46.88	59.75	62.94	45.67	45.49	50.19
100 %	34.50	65.43	94.50	94.50	62.02	64.68	72.59
I 200/100/10/6, $l = 5000\,mm$							
50 %	17.97	18.35	18.46	18.95	18.42	17.49	17.58
60 %	21.56	22.77	23.31	24.48	22.90	21.54	21.89
70 %	25.16	28.53	30.30	32.51	28.53	26.64	27.63
80 %	28.75	36.67	41.86	45.13	36.26	33.93	36.28
90 %	32.34	48.83	62.24	65.56	47.58	45.49	50.19
100 %	35.94	68.16	98.44	98.44	64.60	64.68	72.59
I 200/150/20/8, $l = 5000\,mm$							
50 %	17.97	18.35	18.46	18.95	18.38	18.18	18.28
60 %	21.56	22.65	23.31	24.48	22.78	22.31	22.66
70 %	25.16	28.06	30.30	32.51	28.23	27.36	28.37
80 %	28.75	35.63	41.86	45.13	35.59	34.36	36.88
90 %	32.34	47.10	62.24	65.56	46.21	45.14	50.64
100 %	35.94	65.61	98.44	98.44	62.04	62.70	73.41

Continued on the next page.

[4]Explanation of I cross-section dimensions: I $h/b/t_f/t_w$

Load step	Elastic defl. (mm)	Abaqus (mm)	Eurocode (mm)	R&M (mm)	R&M mod. (mm)	CECS 410 (mm)	New method (mm)
H 200/200/20/10, $l = 6000\,mm$							
50 %	25.88	26.42	26.58	27.28	26.47	26.18	26.32
60 %	31.05	32.62	33.57	35.25	32.82	32.14	32.63
70 %	36.23	40.41	43.64	46.81	40.70	39.42	40.87
80 %	41.40	51.34	60.27	64.99	51.37	49.55	53.15
90 %	46.58	67.94	89.62	94.40	66.79	65.16	73.05
100 %	51.75	94.87	141.75	141.75	89.78	90.60	106.02
H 300/300/30/8, $l = 6000\,mm$							
50 %	17.25	17.60	17.72	18.19	17.68	17.46	17.55
60 %	20.70	21.74	22.38	23.50	21.99	21.47	21.78
70 %	24.15	26.97	29.09	31.21	27.40	26.41	27.32
80 %	27.60	34.40	40.18	43.33	34.84	33.36	35.65
90 %	31.05	46.03	59.75	62.94	45.73	44.20	49.29
100 %	34.50	65.23	94.50	94.50	62.13	61.98	72.22
I 450/150/20/8, $l = 7000\,mm$							
50 %	15.65	15.99	16.08	16.50	16.06	15.87	15.96
60 %	18.78	19.86	20.31	21.32	19.99	19.58	19.89
70 %	21.91	24.93	26.40	28.32	24.96	24.25	25.13
80 %	25.04	32.12	36.46	39.32	31.82	30.99	33.08
90 %	28.18	42.90	54.22	57.11	41.92	41.75	45.88
100 %	31.31	60.12	85.75	85.75	57.17	59.68	66.53
H 500/300/30/15, $l = 8000\,mm$							
50 %	18.40	18.79	18.90	19.40	18.89	18.66	18.76
60 %	22.08	23.31	23.87	25.07	23.53	23.00	23.36
70 %	25.76	29.17	31.03	33.29	29.42	28.48	29.48
80 %	29.44	37.62	42.86	46.22	37.58	36.36	38.79
90 %	33.12	50.50	63.73	67.13	49.63	48.91	53.95
100 %	36.80	71.25	100.80	100.80	67.87	69.82	78.79
H 200/200/30/15, $l = 5000\,mm$							
50 %	17.97	18.46	18.46	18.95	18.27	18.12	18.22
60 %	21.56	22.63	23.31	24.48	22.46	22.11	22.46
70 %	25.16	27.64	30.30	32.51	27.41	26.76	27.78
80 %	28.75	34.34	41.86	45.13	33.77	32.82	35.41
90 %	32.34	44.24	62.24	65.56	42.52	41.64	47.40
100 %	35.94	59.52	98.44	98.44	55.09	55.37	66.99

Table 28: Deflection of simply supported beams subjected to uniform bending moment - hollow sections[5](1.4301)

Load step	Elastic defl. (mm)	Abaqus (mm)	Eurocode (mm)	R&M (mm)	R&M mod. (mm)	New method (mm)
RHS 100/50/4, $l = 3000\,mm$						
50 %	12.94	13.19	13.29	13.64	13.12	13.14
60 %	15.53	16.30	16.78	17.62	16.07	16.25
70 %	18.11	20.14	21.82	23.41	19.49	20.18
80 %	20.70	25.08	30.14	32.50	23.77	25.73
90 %	23.29	31.65	44.81	47.20	29.51	33.96
100 %	25.88	41.08	70.88	70.88	37.59	46.09
RHS 120/80/5, $l = 3000\,mm$						
50 %	10.78	11.00	11.07	11.37	10.96	10.96
60 %	12.94	13.61	13.99	14.69	13.48	13.59
70 %	15.09	16.89	18.18	19.51	16.45	16.96
80 %	17.25	21.21	25.11	27.08	20.28	21.82
90 %	19.41	27.11	37.34	39.34	25.55	29.19
100 %	21.56	35.80	59.06	59.06	33.12	40.31
RHS 160/80/5, $l = 5000\,mm$						
50 %	22.46	22.90	23.07	23.68	22.80	22.83
60 %	26.95	28.35	29.14	30.60	27.96	28.24
70 %	31.45	35.09	37.88	40.64	33.99	35.15
80 %	35.94	43.83	52.32	56.42	41.60	44.93
90 %	40.43	55.46	77.80	81.95	51.91	59.48
100 %	44.92	72.36	123.05	123.05	66.52	81.07
RHS 200/120/8, $l = 5000\,mm$						
50 %	17.97	18.33	18.46	18.95	18.25	18.27
60 %	21.56	22.68	23.31	24.48	22.41	22.62
70 %	25.16	28.10	30.30	32.51	27.30	28.19
80 %	28.75	35.19	41.86	45.13	33.54	36.17
90 %	32.34	44.77	62.24	65.56	42.05	48.17
100 %	35.94	58.81	98.44	98.44	54.20	66.13

Continued on the next page.

[5]Explanation of hollow cross-section dimensions: RHS $h/b/t$; SHS h/t

Load step	Elastic defl. (mm)	Abaqus (mm)	Eurocode (mm)	R&M (mm)	R&M mod. (mm)	New method (mm)
RHS 250/100/6, $l = 5000\,mm$						
50 %	14.38	14.65	14.77	15.16	14.57	14.60
60 %	17.25	18.13	18.65	19.58	17.84	18.04
70 %	20.13	22.40	24.24	26.01	21.61	22.38
80 %	23.00	27.85	33.49	36.11	26.30	28.44
90 %	25.88	34.97	49.79	52.45	32.57	37.33
100 %	28.75	45.18	78.75	78.75	41.35	50.39
RHS 300/200/10, $l = 6000\,mm$						
50 %	17.25	17.60	17.72	18.19	17.56	17.55
60 %	20.70	21.82	22.38	23.50	21.61	21.77
70 %	24.15	27.13	29.09	31.21	26.45	27.22
80 %	27.60	34.17	40.18	43.33	32.72	35.11
90 %	31.05	43.87	59.75	62.94	41.43	47.12
100 %	34.50	58.14	94.50	94.50	54.04	65.32
RHS 400/200/12, $l = 7000\,mm$						
50 %	17.61	17.95	18.09	18.57	17.88	17.90
60 %	21.13	22.23	22.85	23.99	21.93	22.15
70 %	24.65	27.53	29.70	31.86	26.66	27.57
80 %	28.18	34.40	41.02	44.23	32.65	35.25
90 %	31.70	43.55	60.99	64.25	40.77	46.69
100 %	35.22	56.85	96.47	96.47	52.30	63.68
SHS 60/4, $l = 3000\,mm$						
50 %	21.56	22.03	22.15	22.73	21.95	21.93
60 %	25.88	27.24	27.97	29.37	27.03	27.17
70 %	30.19	33.69	36.36	39.01	33.10	33.96
80 %	34.50	42.43	50.23	54.16	40.98	43.83
90 %	38.81	54.72	74.68	78.67	51.95	59.14
100 %	43.13	73.20	118.13	118.13	67.84	82.83
SHS 100/5, $l = 3000\,mm$						
50 %	12.94	13.21	13.29	13.64	13.19	13.17
60 %	15.53	16.36	16.78	17.62	16.29	16.35
70 %	18.11	20.36	21.82	23.41	20.05	20.51
80 %	20.70	25.82	30.14	32.50	25.02	26.62
90 %	23.29	33.58	44.81	47.20	32.04	36.15
100 %	25.88	45.36	70.88	70.88	42.35	50.96

Continued on the next page.

Load step	Elastic defl. (mm)	Abaqus (mm)	Eurocode (mm)	R&M (mm)	R&M mod. (mm)	New method (mm)
SHS 150/16, $l = 4000\,mm$						
50 %	15.33	15.75	15.75	16.17	15.55	15.56
60 %	18.40	19.39	19.89	20.89	19.04	19.20
70 %	21.47	23.79	25.86	27.74	23.08	23.80
80 %	24.53	29.59	35.72	38.51	28.14	30.35
90 %	27.60	37.57	53.11	55.94	34.90	40.36
100 %	30.67	49.08	84.00	84.00	44.41	55.79
SHS 160/10, $l = 4000\,mm$						
50 %	14.38	14.68	14.77	15.16	14.64	14.62
60 %	17.25	18.16	18.65	19.58	18.04	18.13
70 %	20.13	22.49	24.24	26.01	22.12	22.67
80 %	23.00	28.39	33.49	36.11	27.43	29.31
90 %	25.88	36.67	49.79	52.45	34.86	39.61
100 %	28.75	49.12	78.75	78.75	45.67	55.56
SHS 200/6, $l = 5000\,mm$						
50 %	17.97	18.34	18.46	18.95	18.37	18.32
60 %	21.56	22.82	23.31	24.48	22.78	22.79
70 %	25.16	28.58	30.30	32.51	28.21	28.72
80 %	28.75	36.50	41.86	45.13	35.56	37.55
90 %	32.34	47.98	62.24	65.56	46.16	51.42
100 %	35.94	65.81	98.44	98.44	61.93	73.13
SHS 200/16, $l = 5000\,mm$						
50 %	17.97	18.38	18.46	18.95	18.26	18.26
60 %	21.56	22.69	23.31	24.48	22.45	22.60
70 %	25.16	27.99	30.30	32.51	27.39	28.15
80 %	28.75	35.08	41.86	45.13	33.72	36.19
90 %	32.34	45.03	62.24	65.56	42.42	48.59
100 %	35.94	59.76	98.44	98.44	54.89	67.73
SHS 400/10, $l = 7000\,mm$						
50 %	17.61	17.98	18.09	18.57	18.02	17.96
60 %	21.13	22.40	22.85	23.99	22.36	22.36
70 %	24.65	28.08	29.70	31.86	27.75	28.21
80 %	28.18	35.94	41.02	44.23	35.07	36.95
90 %	31.70	47.36	60.99	64.25	45.68	50.71
100 %	35.22	65.19	96.47	96.47	61.53	72.29

Table 29: Deflection of simply supported beams subjected to uniform bending moment - T-sections[6](1.4301)

Load step	Elastic defl. (mm)	Abaqus (mm)	Eurocode (mm)	New method (mm)
T 200/100/10, $l = 5000\,mm$				
50 %	13.88	13.99	14.25	13.92
60 %	16.65	16.96	18.00	16.82
70 %	19.43	20.11	23.40	19.91
80 %	22.20	23.57	32.33	23.42
90 %	24.98	27.49	48.07	27.69
100 %	27.75	32.12	76.02	33.24
T 100/100/10, $l = 4000\,mm$				
50 %	16.13	16.36	16.56	16.18
60 %	19.35	19.84	20.92	19.54
70 %	22.58	23.58	27.19	23.13
80 %	25.80	27.74	37.56	27.20
90 %	29.03	32.49	55.85	32.15
100 %	32.25	38.12	88.34	38.52
T 300/100/12, $l = 6000\,mm$				
50 %	14.17	14.28	14.55	14.22
60 %	17.00	17.31	18.38	17.19
70 %	19.83	20.56	23.89	20.39
80 %	22.67	24.15	33.00	24.07
90 %	25.50	28.29	49.06	28.66
100 %	28.33	33.36	77.60	34.84
T 450/150/15, $l = 6000\,mm$				
50 %	9.40	9.47	9.66	9.44
60 %	11.28	11.49	12.20	11.41
70 %	13.16	13.64	15.86	13.53
80 %	15.04	16.02	21.90	15.97
90 %	16.92	18.76	32.57	19.02
100 %	18.81	22.12	51.51	23.11

[6]Explanation of T-section dimensions: T $h/b/t$

Table 30: Deflection of simply supported beams subjected to uniform bending moment - asymmetrical I sections[7](1.4301)

Load step	Elastic defl. (mm)	Abaqus (mm)	Eurocode (mm)	New method (mm)
I 200/200/100/20/10, $l = 6000\,mm$				
50 %	20.92	21.30	21.49	21.13
60 %	25.10	26.03	27.14	25.85
70 %	29.29	31.50	35.28	31.42
80 %	33.47	38.30	48.73	38.61
90 %	37.66	47.31	72.46	48.32
100 %	41.84	59.82	114.61	61.33
I 300/300/100/20/10, $l = 6000\,mm$				
50 %	12.76	12.96	13.10	12.90
60 %	15.31	15.87	16.55	15.81
70 %	17.86	19.26	21.51	19.28
80 %	20.41	23.46	29.72	23.77
90 %	22.96	28.98	44.19	29.78
100 %	25.51	36.48	69.89	37.59
I 450/200/100/15/8, $l = 6000\,mm$				
50 %	9.71	9.83	9.97	9.82
60 %	11.65	12.04	12.60	12.03
70 %	13.59	14.59	16.37	14.67
80 %	15.53	17.71	22.62	18.10
90 %	17.48	21.80	33.63	22.76
100 %	19.42	27.50	53.19	29.14
I 450/300/100/15/8, $l = 7000\,mm$				
50 %	11.95	12.10	12.27	12.08
60 %	14.34	14.82	15.50	14.80
70 %	16.73	17.94	20.15	18.03
80 %	19.12	21.69	27.84	22.16
90 %	21.51	26.48	41.39	27.59
100 %	23.90	32.82	65.47	34.58

[6]Explanation of asymmetrical I cross-section dimensions: I $h/b_1/b_2/t_f/t_w$

Table 31: Deflection of simply supported beams subjected to a concentrated load at mid-span - I sections (1.4301)

Load step	Elastic defl. (mm)	Abaqus (mm)	Eurocode (mm)	R&M (mm)	R&M mod. (mm)	CECS 410 (mm)	New method (mm)
I 200/100/10/6, $l = 5000\,mm$							
50 %	11.98	12.31	12.30	12.22	12.09	12.03	12.06
60 %	14.38	14.95	15.54	15.10	14.71	14.57	14.67
70 %	16.77	17.89	20.20	18.61	17.61	17.35	17.63
80 %	19.17	21.42	27.90	23.26	21.05	20.63	21.33
90 %	21.56	25.94	41.49	29.87	25.37	24.90	26.44
100 %	23.96	32.13	65.63	39.58	31.12	30.94	33.94
I 450/150/20/8, $l = 10000\,mm$							
50 %	21.30	22.00	21.88	21.73	21.50	21.40	21.44
60 %	25.56	26.72	27.63	26.85	26.17	25.92	26.09
70 %	29.81	31.99	35.92	33.08	31.37	30.87	31.37
80 %	34.07	38.34	49.61	41.36	37.53	36.77	38.01
90 %	38.33	46.51	73.76	53.10	45.35	44.49	47.18
100 %	42.59	57.71	116.67	70.37	55.79	55.46	60.68
I 300/300/30/8, $l = 7000\,mm$							
50 %	15.65	16.20	16.08	15.97	15.80	15.72	15.75
60 %	18.78	19.63	20.31	19.74	19.22	19.02	19.13
70 %	21.91	23.39	26.40	24.32	23.02	22.60	22.93
80 %	25.04	27.85	36.46	30.40	27.51	26.79	27.62
90 %	28.18	33.61	54.22	39.03	33.17	32.15	34.04
100 %	31.31	41.65	85.75	51.72	40.71	39.62	43.52
I 200/200/20/10, $l = 7000\,mm$							
50 %	23.48	23.99	24.12	23.96	23.68	23.57	23.62
60 %	28.18	29.06	30.46	29.60	28.78	28.50	28.68
70 %	32.87	34.63	39.60	36.47	34.39	33.84	34.36
80 %	37.57	41.20	54.69	45.59	40.96	40.03	41.34
90 %	42.26	49.61	81.32	58.54	49.14	47.88	50.84
100 %	46.96	61.17	128.63	77.58	59.90	58.71	64.75

Table 32: Deflection of simply supported beams subjected to a concentrated load at mid-span - hollow sections (1.4301)

Load step	Elastic defl. (mm)	Abaqus (mm)	Eurocode (mm)	R&M (mm)	R&M mod. (mm)	New method (mm)
RHS 120/80/5, $l = 5000\,mm$						
50 %	19.97	20.24	20.51	20.37	20.09	20.08
60 %	23.96	24.56	25.90	25.17	24.33	24.38
70 %	27.95	29.33	33.67	31.02	28.90	29.19
80 %	31.94	34.87	46.51	38.77	34.05	35.06
90 %	35.94	41.64	69.15	49.78	40.20	42.86
100 %	39.93	50.29	109.38	65.97	47.96	53.80
RHS 200/120/8, $l = 6000\,mm$						
50 %	17.25	17.57	17.72	17.60	17.35	17.35
60 %	20.70	21.32	22.38	21.75	21.01	21.06
70 %	24.15	25.44	29.09	26.80	24.92	25.20
80 %	27.60	30.22	40.18	33.50	29.32	30.23
90 %	31.05	36.02	59.75	43.01	34.54	36.88
100 %	34.50	43.35	94.50	57.00	41.07	46.15
RHS 300/200/10, $l = 7000\,mm$						
50 %	15.65	16.06	16.08	15.97	15.76	15.75
60 %	18.78	19.49	20.31	19.74	19.09	19.13
70 %	21.91	23.29	26.40	24.32	22.70	22.92
80 %	25.04	27.72	36.46	30.40	26.79	27.56
90 %	28.18	33.14	54.22	39.03	31.71	33.75
100 %	31.31	40.10	85.75	51.72	37.95	42.47
SHS 100/5, $l = 4000\,mm$						
50 %	15.33	15.57	15.75	15.65	15.45	15.43
60 %	18.40	18.90	19.89	19.33	18.74	18.75
70 %	21.47	22.58	25.86	23.82	22.33	22.48
80 %	24.53	26.92	35.72	29.78	26.45	27.09
90 %	27.60	32.34	53.11	38.23	31.49	33.31
100 %	30.67	39.46	84.00	50.67	37.99	42.22

Continued on the next page.

Load step	Elastic defl. (mm)	Abaqus (mm)	Eurocode (mm)	R&M (mm)	R&M mod. (mm)	New method (mm)
SHS 150/16, $l = 6000\,mm$						
50 %	23.00	23.57	23.63	23.47	23.12	23.12
60 %	27.60	28.53	29.84	29.00	27.96	28.02
70 %	32.20	33.89	38.79	35.73	33.11	33.44
80 %	36.80	40.05	53.58	44.66	38.83	39.94
90 %	41.40	47.49	79.66	57.34	45.51	48.47
100 %	46.00	56.93	126.00	76.00	53.73	60.42
SHS 400/10, $l = 8000\,mm$						
50 %	15.33	15.88	15.75	15.65	15.47	15.44
60 %	18.40	19.30	19.89	19.33	18.80	18.78
70 %	21.47	23.12	25.86	23.82	22.48	22.57
80 %	24.53	27.68	35.72	29.78	26.79	27.32
90 %	27.60	33.44	53.11	38.23	32.17	33.82
100 %	30.67	41.15	84.00	50.67	39.26	43.23

Table 33: Deflection of simply supported beams subjected to a uniformly distributed load - I sections (1.4301)

Load step	Elastic defl. (mm)	Abaqus (mm)	Eurocode (mm)	R&M (mm)	R&M mod. (mm)	CECS 410 (mm)	New method (mm)
I 200/100/10/6, $l = 5000\,mm$							
50 %	14.97	15.41	15.38	15.51	15.22	15.10	15.16
60 %	17.97	18.89	19.43	19.56	18.70	18.42	18.64
70 %	20.96	23.05	25.25	24.98	22.80	22.29	22.93
80 %	23.96	28.50	34.88	32.90	28.06	27.34	28.89
90 %	26.95	36.11	51.86	45.08	35.27	34.65	37.95
100 %	29.95	47.42	82.03	64.06	45.60	46.05	52.13
I 450/150/20/8, $l = 10000\,mm$							
50 %	26.62	27.51	27.34	27.57	27.07	26.85	26.96
60 %	31.94	33.74	34.54	34.77	33.29	32.77	33.16
70 %	37.27	41.22	44.89	44.40	40.66	39.71	40.83
80 %	42.59	51.04	62.01	58.49	50.15	48.81	51.54
90 %	47.92	64.80	92.20	80.15	63.23	62.10	67.86
100 %	53.24	85.36	145.83	113.89	82.05	82.90	93.43
I 300/300/30/8, $l = 7000\,mm$							
50 %	19.57	20.24	20.10	20.26	19.89	19.72	19.79
60 %	23.48	24.71	25.38	25.56	24.44	24.02	24.27
70 %	27.39	29.95	33.00	32.64	29.81	28.97	29.72
80 %	31.31	36.77	45.58	42.99	36.69	35.32	37.23
90 %	35.22	46.54	67.77	58.91	46.13	44.38	48.67
100 %	39.13	61.52	107.19	83.71	59.66	58.29	67.04
I 200/200/20/10, $l = 7000\,mm$							
50 %	29.35	30.05	30.15	30.39	29.79	29.56	29.67
60 %	35.22	36.69	38.08	38.34	36.54	35.98	36.38
70 %	41.09	44.45	49.50	48.96	44.41	43.32	44.50
80 %	46.96	54.48	68.37	64.49	54.37	52.64	55.62
90 %	52.83	68.60	101.65	88.36	67.85	65.78	72.42
100 %	58.70	89.84	160.78	125.57	86.96	85.78	99.11

Table 34: Deflection of simply supported beams subjected to a uniformly distributed load - hollow sections (1.4301)

Load step	Elastic defl. (mm)	Abaqus (mm)	Eurocode (mm)	R&M (mm)	R&M mod. (mm)	New method (mm)
RHS 120/80/5, $l = 4000\,mm$						
50 %	15.97	16.30	16.41	16.54	16.15	16.15
60 %	19.17	19.95	20.72	20.86	19.69	19.79
70 %	22.36	24.22	26.94	26.64	23.68	24.17
80 %	25.56	29.54	37.21	35.10	28.50	30.05
90 %	28.75	36.45	55.32	48.09	34.71	38.54
100 %	31.94	45.98	87.50	68.34	43.16	51.09
RHS 200/120/8, $l = 6000\,mm$						
50 %	21.56	22.03	22.15	22.33	21.79	21.79
60 %	25.88	26.96	27.97	28.17	26.54	26.70
70 %	30.19	32.70	36.36	35.97	31.88	32.58
80 %	34.50	39.81	50.23	47.38	38.26	40.41
90 %	38.81	48.98	74.68	64.92	46.44	51.67
100 %	43.13	61.49	118.13	92.25	57.48	68.17
RHS 300/200/10, $l = 7000\,mm$						
50 %	19.57	20.11	20.10	20.26	19.79	19.79
60 %	23.48	24.63	25.38	25.56	24.16	24.27
70 %	27.39	29.94	33.00	32.64	29.10	29.67
80 %	31.31	36.58	45.58	42.99	35.11	36.96
90 %	35.22	45.25	67.77	58.91	42.93	47.54
100 %	39.13	57.24	107.19	83.71	53.65	63.21
SHS 100/5, $l = 4000\,mm$						
50 %	19.17	19.54	19.69	19.85	19.42	19.39
60 %	23.00	23.92	24.87	25.04	23.75	23.80
70 %	26.83	29.10	32.32	31.97	28.71	29.15
80 %	30.67	35.69	44.65	42.11	34.86	36.45
90 %	34.50	44.54	66.39	57.71	43.00	47.24
100 %	38.33	57.12	105.00	82.00	54.32	63.63

Continued on the next page.

Load step	Elastic defl. (mm)	Abaqus (mm)	Eurocode (mm)	R&M (mm)	R&M mod. (mm)	New method (mm)
SHS 150/16, $l = 6000\,mm$						
50 %	28.75	29.54	29.53	29.77	29.01	29.02
60 %	34.50	35.99	37.30	37.56	35.29	35.48
70 %	40.25	43.37	48.49	47.96	42.24	43.10
80 %	46.00	52.45	66.97	63.17	50.42	53.15
90 %	51.75	64.25	99.58	86.56	60.72	67.64
100 %	57.50	80.31	157.50	123.00	74.38	89.36
SHS 400/10, $l = 8000\,mm$						
50 %	19.17	19.85	19.69	19.85	19.46	19.41
60 %	23.00	24.38	24.87	25.04	23.88	23.87
70 %	26.83	29.79	32.32	31.97	29.04	29.36
80 %	30.67	36.77	44.65	42.11	35.58	36.97
90 %	34.50	46.29	66.39	57.71	44.47	48.36
100 %	38.33	60.12	105.00	82.00	57.09	65.80

Table 35: Deflection of simply supported beams subjected to two concentrated loads at thirds of the span (1.4301)

Load step	Elastic defl. (mm)	Abaqus (mm)	Eurocode (mm)	New method (mm)
I 200/100/10/6, $l = 7000\,mm$				
50 %	30.00	30.74	30.82	30.40
60 %	36.00	37.86	38.92	37.43
70 %	42.00	46.69	50.60	46.19
80 %	48.00	58.63	69.89	58.51
90 %	54.00	75.82	103.91	77.37
100 %	60.00	102.26	164.35	106.99
I 450/150/15/8, $l = 10000\,mm$				
50 %	27.21	28.17	27.95	27.61
60 %	32.65	34.76	35.30	34.06
70 %	38.10	42.91	45.89	42.18
80 %	43.54	53.82	63.39	53.70
90 %	48.98	69.34	94.25	71.30
100 %	54.42	93.00	149.07	98.47
I 200/200/25/15, $l = 7000\,mm$				
50 %	30.00	30.87	30.82	30.34
60 %	36.00	37.72	38.92	37.22
70 %	42.00	45.84	50.60	45.57
80 %	48.00	56.45	69.89	57.06
90 %	54.00	71.50	103.91	74.52
100 %	60.00	94.17	164.35	102.42
I 200/200/40/6, $l = 7000\,mm$				
50 %	30.00	31.13	30.82	30.25
60 %	36.00	37.82	38.92	36.91
70 %	42.00	45.35	50.60	44.66
80 %	48.00	54.68	69.89	54.77
90 %	54.00	67.40	103.91	69.43
100 %	60.00	86.08	164.35	92.22

Continued on the next page.

Load step	Elastic defl. (mm)	Abaqus (mm)	Eurocode (mm)	New method (mm)
RHS 250/100/6, $l = 7000\,mm$				
50 %	24.00	24.56	24.65	24.27
60 %	28.80	30.20	31.14	29.74
70 %	33.60	36.86	40.48	36.29
80 %	38.40	45.09	55.91	44.93
90 %	43.20	55.59	83.13	56.97
100 %	48.00	70.09	131.48	73.80
RHS 200/100/8, $l = 7000\,mm$				
50 %	30.00	30.65	30.82	30.34
60 %	36.00	37.62	38.92	37.22
70 %	42.00	45.92	50.60	45.52
80 %	48.00	56.25	69.89	56.62
90 %	54.00	69.61	103.91	72.44
100 %	60.00	88.14	164.35	95.18
RHS 400/200/8, $l = 10000\,mm$				
50 %	30.61	31.44	31.45	30.98
60 %	36.74	38.72	39.72	38.04
70 %	42.86	47.43	51.63	46.61
80 %	48.98	58.42	71.31	58.12
90 %	55.10	72.80	106.03	74.48
100 %	61.23	92.91	167.71	97.76
RHS 100/100/10, $l = 5000\,mm$				
50 %	30.61	31.41	31.45	30.96
60 %	36.74	38.45	39.72	37.96
70 %	42.86	46.72	51.63	46.43
80 %	48.98	57.22	71.31	57.96
90 %	55.10	71.24	106.03	75.07
100 %	61.23	90.96	167.71	101.38

Table 36: Deflection of simply supported beams subjected to uniform bending moment (1.4003)

Load step	Elastic defl. (mm)	Abaqus (mm)	Eurocode (mm)	R&M (mm)	R&M mod. (mm)	New method (mm)
I 200/100/10/6, $l = 5000\,mm$						
50 %	21.88	21.92	21.88	21.88	21.88	21.88
60 %	26.25	26.33	26.30	26.33	26.27	26.28
70 %	30.63	30.90	31.05	31.23	30.77	30.86
80 %	35.00	36.39	37.75	38.44	35.82	36.52
90 %	39.38	45.44	53.67	55.26	43.16	47.07
100 %	43.75	62.04	106.25	106.25	58.62	74.61
H 300/300/30/30, $l = 6000\,mm$						
50 %	21.00	21.18	21.00	21.01	21.00	21.00
60 %	25.20	25.43	25.25	25.28	25.21	25.22
70 %	29.40	29.77	29.81	29.98	29.48	29.55
80 %	33.60	34.63	36.24	36.90	34.06	34.57
90 %	37.80	41.65	51.53	53.05	39.94	42.80
100 %	42.00	54.74	102.00	102.00	50.41	63.00
RHS 120/80/5, $l = 3000\,mm$						
50 %	13.13	13.16	13.13	13.13	13.13	13.13
60 %	15.75	15.80	15.78	15.80	15.76	15.76
70 %	18.38	18.54	18.63	18.74	18.42	18.50
80 %	21.00	21.82	22.65	23.06	21.26	21.80
90 %	23.63	26.71	32.20	33.16	24.81	27.55
100 %	26.25	34.32	63.75	63.75	30.90	40.63
RHS 200/120/8, $l = 5000\,mm$						
50 %	21.88	21.93	21.88	21.88	21.88	21.88
60 %	26.25	26.34	26.30	26.33	26.26	26.27
70 %	30.63	30.90	31.05	31.23	30.69	30.83
80 %	35.00	36.36	37.75	38.44	35.39	36.30
90 %	39.38	44.41	53.67	55.26	41.18	45.76
100 %	43.75	56.69	106.25	106.25	50.84	66.78

Table 37: Deflection of simply supported beams subjected to uniform bending moment (1.4462)

Load step	Elastic defl. (mm)	Abaqus (mm)	Eurocode (mm)	R&M (mm)	R&M mod. (mm)	New method (mm)
I 200/100/10/6, $l = 5000\,mm$						
50 %	37.50	37.75	37.74	37.99	37.75	37.67
60 %	45.00	45.80	46.05	46.75	45.91	45.72
70 %	52.50	54.96	56.10	57.65	55.18	54.96
80 %	60.00	66.63	70.49	73.11	66.83	67.10
90 %	67.50	83.02	94.40	97.39	83.08	85.38
100 %	75.00	107.13	137.50	137.50	107.58	115.12
H 300/300/30/30, $l = 6000\,mm$						
50 %	36.00	36.43	36.23	36.47	36.17	36.13
60 %	43.20	44.06	44.21	44.88	43.82	43.76
70 %	50.40	52.48	53.86	55.34	52.24	52.33
80 %	57.60	62.76	67.67	70.18	62.27	63.20
90 %	64.80	76.75	90.63	93.50	75.46	78.99
100 %	72.00	97.05	132.00	132.00	94.29	104.27
RHS 120/80/5, $l = 3000\,mm$						
50 %	22.50	22.65	22.65	22.79	22.63	22.59
60 %	27.00	27.47	27.63	28.05	27.45	27.38
70 %	31.50	32.89	33.66	34.59	32.83	32.78
80 %	36.00	39.57	42.29	43.86	39.38	39.65
90 %	40.50	48.30	56.64	58.44	48.22	49.51
100 %	45.00	59.99	82.50	82.50	61.13	64.57
RHS 200/120/8, $l = 5000\,mm$						
50 %	37.50	37.75	37.74	37.99	37.70	37.64
60 %	45.00	45.77	46.05	46.75	45.73	45.61
70 %	52.50	54.79	56.10	57.65	54.66	54.59
80 %	60.00	65.85	70.49	73.11	65.49	65.94
90 %	67.50	80.19	94.40	97.39	80.03	82.12
100 %	75.00	99.22	137.50	137.50	101.20	106.61